JOURNAL OF INNOVATIVE© TRANSPORTATION

CONTENTS

JOURNAL OF INNOVATIVE TRANSPORTATION

Comparison of elvaloy and styrene-butadiene-styrene added polymer modified bitumen

Murat Vergi Taciroğlu*

Civil Engineering Department, Engineering Faculty, Mersin University, Türkiye

Highlights

- Optimum SBS ratio is in the range of 1.6%-1.8% for B50/70 grade pure bitumen
- Optimum Elvaloy ratio is in the range of 4%-5% for B50/70 grade pure bitumen
- The non-homogeneous dispersion of SBS adversely affects storage stability

Abstract

One of the methods used to produce road pavements resistant to increased traffic volume and harsh environmental conditions is to improve the properties of bituminous binders, such as high temperature resistance and aging resistance, by using various additives. Styrene-Butadiene-Styrene and Elvaloy are two different commercial additives that are frequently used in pavement construction. In this study, the performance of three different B50/70 grade pure bitumens was modified by using Elvaloy at 1.6%, 1.7%, and 1.8%, and five different B50/70 grade pure bitumens were modified using 4.0%, 4.5%, and 5.0% Styrene-Butadiene-Styrene. Penetration, softening point, elastic recovery, flash point, storage stability, dynamic shear rheometer, beam bending rheometer, rotational thin film oven, and pressure aging vessel tests were applied to the binders in accordance with the Polymer Modified Bitumen technical specifications. According to the test results, it was determined that the additive rates for both modifiers are the optimum values in accordance with the specification. The results of the storage stability tests also showed that the non-homogeneous dispersion of the Styrene-Butadiene-Styrene modified binders during mixing had a significant effect on the behaviour of the binder after storage.

Keywords: Polymer Modified bitumen, Styrene-Butadiene-Styrene, Elvaloy

1. Introduction

Bituminous binders are frequently used in bituminous mixtures in the construction of highway pavements due to their good adhesion and viscoelastic behaviour [1]. However, increasing traffic density due to the increase in trade volume and the increase in the number of heavy-loaded vehicles in the traffic causes the road pavements to be exposed to more repetitive heavy axle loads. For this reason, it has become necessary to produce more durable road pavements. One of the most preferred methods for the fabrication of durable bituminous pavement layers is the modification of bitumen binders using various additives [2].

Bitumen modification is generally defined as changing the rheological properties of bitumen by mixing various [3]. With this process, which affects the consistency of the bitumen, the binder hardens, softens, or gains more elasticity. Some polymers compatible with bitumen used as additives reduce the sensitivity of the binder to temperature without harming the behaviour of bitumen at low temperatures [4]. The main contributions of the use of modified bitumen in mixtures on road pavement can be counted as increased resistance to fatigue cracks, increased resistance to rutting deformation, and decreased sensitivity to water [5].

Natural materials such as stone dust, lime, rubber tree sap, and lignin can be used as bitumen modifiers, as well as artificial materials such as polyethylene, acrylics, and

polyvinyl chloride [6]. In some studies, researchers have categorized additives mixed with bitumen as fillers, elastomers, thermosets, fibers, thermoplastics, oxidants, antioxidants, hydrocarbons, anti-skinning agents, and reactive thermopolymers [6-7]. Artificial bitumen additives are generally commercial products. Among commercially produced additives, Styrene-Butadiene-Styrene (SBS) and Elvaloy are products that are frequently used by institutions constructing highways. These additives, which have a certain cost, are also used in academic studies for reasons such as providing economy in bitumen modification or increasing the performance of additive bitumen.

During the modification, some molecular structures in the SBS additive increase in volume and change the properties of pure bitumen [8]. The different molecular structures of the additive give the binder strength and elasticity [9]. Furthermore, SBS modification also affects the morphological structure of bitumen [10]. In modifications made with SBS, the amount of additive is generally limited to between 2% and 5% for economic reasons [11,12]. Elvaloy is an elastomeric thermopolymer added to the bituminous binder between 1.5% and 3% by weight. Due to its molecular structure, Elvaloy causes the binder to turn into a gel consistency when it is mixed into the bituminous binder in more than the necessary amount [13]. For this reason, lower amounts of Elvaloy are used as a modifier in studies compared to SBS. According to laboratory tests, bitumen modified with Elvaloy showed superior resistance to deformations and fatigue cracking [11].

Güngör et al. [14], stated that the properties of pure bitumen from different refineries are determinative on the performance of modified bitumen with SBS and Elvaloy additives. Geçgil and Seloğlu [15] prepared modified binders by adding Elvaloy at the rates of 0.5%, 0.75% and 1% to pure B 100/150 grade bitumen. According to the test results, the researchers found that the binders with soft consistency and high temperature sensitivity became harder with the addition of Elvaloy, the binder class changed and the temperature sensitivity decreased significantly. Kumandaş et al. [16] stated that the addition of Elvaloy has positive contributions to the high-temperature performance of bitumen, according to the results of DSR experiments. Yalçın [12] produced modified bitumen by adding 2%–3% and 4% SBS to B160/220 class pure bitumen, which he obtained from two different refineries, and applied penetration, softening point, viscosity, and DSR tests to modified bitumen. According to the results of the DSR tests, the researcher stated that although the different bitumen used were in the same penetration classes, the complex shear modulus and phase angle values were significantly different and exhibited different elastic behaviours from each other. Gedik [17] prepared concrete asphalt specimens according to the Marshall design method for the wearing course using B70/100 grade bitumen

modified with different rates of SBS. The results showed that asphalt concrete mixtures modified with SBS can be used in cold climate regions.

Aydin et al. [5] investigated the rheological properties of Elvaloy and polyphosphoric acid (PPA)-modified bitumen binder by penetration, softening point, rotational viscosity, and dynamic shear rheometer (DSR) experiments. In the study, both additives were added to B50/70-grade pure bitumen at different rates. According to the results they obtained, the penetration values of the bitumen modified by mixing Elvaloy and PPA decreased and the temperature of the softening point increased. Although the viscosity value of the mixtures decreased, the viscosity value of 3 Pa.s, which is the limit condition for the workability of all binders at 135°C, was not exceeded. The results of the DSR experiments also showed that the addition of Elvaloy increased the $G^*/\sin\delta$ values.

In this study, tests were conducted to evaluate the performance of SBS and Elvaloy additives, which are frequently used in highway construction. The results of penetration, softening point, elastic recovery, flash point, storage stability, dynamic shear rheometer (DSR), beam bending rheometer (BBR), rotational thin film oven (RTFOT), and pressure aging vessel (PAV) tests applied to determine the usability of polymer-modified bitumen (PMB) prepared by adding SBS and Elvaloy at different rates were compared. According to the results obtained, it has been determined that PMBs that meet the required specification values can be produced by adding 1.6%, 1.7%, and 1.8% Elvaloy and 4%, 4.5%, and 5% SBS additives to B50/70 grade pure bitumen. Especially when the storage stability test results are examined, it has been determined that in cases where high amounts of SBS-added bitumen need to be stored due to the size of the road construction to be made, modification processes should be done carefully in order to provide homogeneous mixtures during the PMB preparation stage.

2 Material and Methods

The B 50/70 grade pure bitumen used in the modification in this study was produced in the Aliağa refinery. The bitumen performance tests specified in the "Polymer Modified Bitumen (PMB) Technical Specification" were applied to the samples obtained by mixing Elvaloy and SBS additives with bitumen. While preparing modified bitumen with SBS, pure bitumen was heated at 180 °C for 1 hour before adding the modifier material. Then, SBS was added in such a way that there was no agglomeration, and it was mixed mechanically at 1000 rpm rotation speed, 170 °C, and for 1 hour. Polymer-modified bitumen prepared with Elvaloy was preheated at 180 °C for 1 hour, and then Elvaloy additives were added and mixed mechanically for 8 hours at an 800 rpm rotation speed.

Table 1 shows the tests and specifications applied to modified bitumen.

Table 1. Tests and standards applied to modified bitumen [18-28]

Test	Specification
Penetration	TS EN 1426
Softening Point	TS EN 1427
Elastic Recovery	TS EN 13398
Flash Point	TS EN ISO 2592
Specific Gravity	TS EN 15326+A1
Storage Stability	TS EN 13399
Dynamic Shear Rheometer (DSR)	TS EN 14770
Bending Beam Rhometer (BBR)	TS EN 14771
	ASTM D 6648
Rotional Thin Film Owen (RTFOT)	TS EN 12607-1
	AASHTO T 240
Pressure Aging Vessel (PAV)	TS EN 14769

The tests given above were applied to 1.6%, 1.7% and 1.8% Elvaloy doped PMBs and 4%, 4.5% and 5% SBS doped PMBs. These ratios were determined by taking into account the recommendations of the additive producer companies.

3. Results and Discussions

In this study, the results of 3 different PMB modified with Elvaloy and 5 different PMB modified with SBS were examined.

3.1. Test results of Elvaloy modified binders

In Table 2, the results of traditional bitumen tests applied to three different bitumen binders of the B 50/70 grade modified with Elvaloy are summarized. According to the results of the penetration tests, as the Elvaloy content in all modified bitumen increases, the penetration depth decreases, and the binders acquire a harder consistency, although there is no significant difference. Similar results were observed in the softening point experiments: as the additive ratio increased, the softening point temperatures of the modified bitumens increased. As the Elvaloy ratio increased, the penetration index for B2 binder decreased, while the penetration index for B1 and B3 binders increased. According to the flash point test results, an increase of at least 5 °C was observed in the ignition temperatures of the binders as the Elvaloy ratio

increased. While the specific gravity values, which are an important calculation parameter in the calculations of bituminous mixtures, did not show any change for the B2 binder as the Elvaloy content increased, it caused a decrease in the specific gravity of B1 and an increase in the specific gravity of B3. The specific gravity values calculated for the three binders are generally compatible with the bitumen specific gravity values, which are considered to be between 1.00 and 1.10. According to the results of the elastic recovery test of the modified bituminous binders, as the Elvaloy ratio increases for the B1 and B2 binders, the elastic recovery gain decreases, while it increases for the B3 binder.

The findings of the softening point and penetration tests applied to the top and bottom halves of the Elvaloy modified binders subjected to the storage stability test are summarized in Table 3. It was determined that the bitumen modified according to the differences between the penetration and softening point values of the top and bottom halves of three different samples, which were close to each other, formed a mixture close to homogeneous. According to the test results before and after storage, it was concluded that the softening point temperature and penetration values of the stored modified bitumen decreased, and according to these results, the binders aged to a certain extent during storage.

The results of the RTFOT tests and the penetration and softening point tests applied to the samples after RTFOT are summarized in Table 4. It was determined that the changes in the Elvaloy ratio in the mixtures made with each different bitumen sample did not affect the material loss after the RFTOT test. The softening point temperatures after RTFOT increased with the increase in the additive ratio for all three modified binders. Permanent penetration percentage after RTFOT increased as the Elvaloy content increased in B2 and B3 binders, while it decreased with the increase in Elvaloy content in the B1 binder. In the mixtures created by mixing 1.8% Elvaloy with B1 and B2 bitumens, the increase in softening point temperature after RTFOT exceeded the maximum 8 °C difference recommended in the "Polymer Modified Bitumen (PMB) Technical Specifications" [29]

Table 2. Results of conventional bitumen tests for Elvaloy modified binders

Binder	Elvaloy Content (%)	Penetration (0.1 mm)	Softening Point (°C)	Penetration Indeks	Elastic Recovery (%)	Flash Point (°C)	Specific Gravity
B1	1.7	47.6	65.25	1.89	48.0	307.5	1.046
	1.8	45.8	67.35	2.16	42.0	317.5	1.039
B2	1.7	40.8	68.20	2.02	76.5	292.5	1.024
	1.8	31.7	65.85	1.04	68.0	302.5	1.024
B3	1.6	45.5	62.30	1.24	63.5	225.0	1.02
	1.7	43.6	64.75	1.58	75.0	230.0	1.037

Table 3. Results of storage stability tests for Elvaloy modified binders

Binder	Elvaloy Content (%)	Softening Point (°C)				Penetration (0.1 mm)			
		SP_{top}	SP_{bottom}	ΔSP	Before storage	P_{top}	P_{bottom}	ΔP	Before storage
B1	1.7	63.8	62.5	1.3	65.25	43.0	41.6	1.4	47.6
	1.8	63.7	63.0	0.7	67.35	43.8	42.5	1.3	45.8
B2	1.7	61.5	60.2	1.3	68.20	35.7	33.1	2.6	40.8
	1.8	65.7	64.3	1.4	65.85	31.4	32.3	0.9	31.7
B3	1.6	61.2	61.3	0.1	62.30	34.3	33.8	0.5	45.5
	1.7	61.8	61.1	0.7	64.75	36.7	35.6	1.1	43.6

Table 4. Results of RTFOT experiments for Elvaloy modified binders

Binder	Elvaloy Content (%)	Mass Loss	After RTFOT		
			Softening Point (°C)	Softening Point Difference (°C)	Permanent Penetration (%)
B1	1.7	0.3	72.25	7.0	62
	1.8	0.3	81.65	14.3	60
B2	1.7	0.3	73.95	5.8	61
	1.8	0.3	75.45	9.6	82.3
B3	1.6	0.03	66.35	4.1	83.7
	1.7	0.03	71.75	7.0	84.2

Table 5. Results of DSR and BBR tests for Elvaloy modified binders

Binder	Elvaloy Content (%)	DSR Failure Temp.(°C)	After RTFOT	After RTFOT and PAV	
			DSR Failure Temp.(°C)	DSR Failure Temp.(°C)	BBR Failure Temp.(°C)
B1	1.7	84.9	88.3	26.2	-6
	1.8	86.2	93.0	26.8	-6
B2	1.7	83.7	89.3	22.7	-6
	1.8	83.0	81.0	22.7	-6
B3	1.6	76.0	75.2	24.6	-6
	1.7	80.4	77.0	23.3	-6

Table 5 summarizes the results of DSR and BBR tests of Elvaloy-added binders. The results of DSR tests before aging, after RTFOT aging, and after PAV aging for all binder samples are given as the failure temperature under loading specified in the test standard. According to the results obtained, as the Elvaloy content increased, the failure temperatures of all samples before and after RTFOT aging increased. After pressure aging, as the Elvaloy content increased, a small increase was observed in the failure temperature for the B1 binder, while no change was observed for the B2 binder. In B3 binder, the increase in Elvaloy content decreased the failure temperature. According to the results of BBR tests, creep hardness values less than 300 MPa and m values greater than 0.300 were reached in all samples at -6 °C.

In the table of "Polymer Modified Bitumen (PMB) Technical Specifications" shown in the book "Bitumen Class Selection Maps for HMA Paved Roads" published by the General Directorate of Highways, there are 3 different types of modified bitumen, PMB 70-16, PMB 76-16, and PMB 82-16, for which BBR values at -6 °C are available. Accordingly, the penetration values of six different samples modified with Elvaloy are suitable for the PMB 70-16, PMB 76-16, and PMB 82-16 grades.

For the softening point values, all samples provided the values of the PMB 70-16 grade, while the B1 sample with

1.8% Elvaloy content and the B2 sample with 1.7% Elvaloy content also provided the limit values for PMB 76-16.

According to the results of the elastic recovery test, B1 binders with 1.7% and 1.8% Elvaloy content could not meet the limit values. The remaining binders meet all recommended values for PMB 70-16, PMB 76-16, and PMB 82-16.

Flash point, specific gravity, and softening point after storage for all samples, as well as the results of penetration tests, provide recommended limit values for PMB 70-16, PMB 76-16, and PMB 82-16.

Measurements of mass loss, softening point, and penetration after short-term aging (RTFOT) provide recommended limit values for PMB 70-16, PMB 76-16, and PMB 82-16. However, when the softening point differences were examined, it was determined that 1.8% Elvaloy added B1 and B2 binders did not provide any PMB limits.

According to the results of DSR tests performed before aging, after RTFOT aging, and after PAV aging of B1 and B2 binders added to 1.7% and 1.8%, Elvaloy provides the recommended breakpoints for PMB 70-16, PMB 76-16, and PMB 82-16. The B3 binder, on the other hand, provides the limit values determined for PMB 70-16 in both Elvaloy contents for DSR tests.

When the results of all tests for PMBs prepared with Elvaloy are examined together, it has been determined that all samples generally provide at least PMB 70-16 grade modified bitumen values.

3.2. Test results of binders modified with SBS

Table 6 shows the results of penetration, softening point, elastic recovery, flash point, and specific gravity tests applied to five different bitumen binders of the B 50/70 grade modified with SBS. As the SBS content in the modified bitumens increased, the penetration depth decreased for the B4, B7, and B8 binders, while limited increases occurred for the B6 and B7 bitumens. On the other hand, the softening point temperatures increased with the increasing amount of SBS in the other 4 binders, except for the B5 binder. Penetration index values generally increased with the increment of SBS ratio. According to the flash point test results, as the SBS ratio changed, close results were obtained in the ignition temperatures of the binders. Although the specific gravity values of SBS-modified bitumen are close to each other, they are compatible with the bitumen specific gravity values between 1.00 and 1.10. According to the results of the elastic recovery test, for B4, B7, and B8 binders, the elastic recovery gains showed limited changes with the amount of SBS, while the elastic recovery value decreased by 18% in the B5 binder and increased by 12.5% in the B6 binder with the increase of the SBS amount from 4% to 4.5%.

The findings of the storage stability test results are summarized in Table 7. It is seen that the difference values of the top and bottom halves of five different samples, which were subjected to both softening point and penetration tests after storage, are well above the limit values allowed in the PMB technical specification. This is due to the fact that the SBS additive brands and pure bitumen used are different from each other. As specified in the PMB technical specification, the results of storage stability tests become important if modified bitumen has to be stored during road construction.

The results of the RTFOT tests applied to the bituminous binders modified with SBS are summarized in Table 8. Accordingly, it was determined that adding SBS to different pure bitumen at the rates specified in the study changed the material loss after the RFTOT test to a limited extent. According to the results of the softening point tests performed after short-term aging, the softening point difference temperatures of the modified bitumen prepared with B5 and B8 binders higher than the limit values given in the PMB technical specifications. In modified binders prepared with B4, B6, and B7 binders, a difference within the limit values recommended in the specification was obtained. Permanent penetration percentages decreased when the SBS ratio was subtracted from 4.5% for B7 and B8 binders and increased with increasing SBS ratios in other binders. Permanent penetration percentages for all binders provide the limit values specified in the specification [29].

Table 6. Results of conventional bitumen tests for SBS modified binders

Binder	SBS Content (%)	Penetration (0.1 mm)	Softening Point (°C)	Penetration Indeks	Elastic Recovery (%)	Flash Point (°C)	Specific Gravity
B4	4.0	35.8	71.20	2.19	80.0	310.0	1.037
	4.5	32.9	73.20	2.31	79.0	315.0	1.020
	5.0	32.5	75.00	2.55	82.0	310.0	1.026
B5	4.0	29.0	88.60	4.07	94.5	310.0	1.030
	4.5	29.4	67.15	1.10	76.5	305.0	1.039
B6	4.0	36.3	75.45	2.87	80.0	312.5	1.038
	4.5	36.6	82.50	3.86	92.5	307.5	1.037
B7	4.5	45.9	98.50	6.27	97.5	312.5	1.031
	5.0	44.9	99.40	6.30	96.5	312.5	1.039
B8	4.5	41.0	85.55	4.53	73.8	302.5	1.039
	5.0	38.0	89.55	4.82	74.0	307.5	1.040

Table 7. Results of storage stability tests for SBS modified binders

Binder	SBS Content (%)	Storage Stability							
		Softening Point (°C)				Penetration (0.1 mm)			
		SPtop	SPbottom	ΔSP	Before storage	Ptop	Pbottom	ΔP	Before storage
B4	4.0	30.6	63.0	32.4	71.20	89.2	22.9	66.3	35.8
	4.5	29.9	62.1	32.2	73.20	88.5	19.0	69.5	32.9
	5.0	31.0	60.2	29.2	75.00	90.1	18.4	71.7	32.5
B5	4.0	30.6	63.0	32.4	88.60	48.5	27.4	21.1	29.0
	4.5	29.9	62.1	32.2	67.15	33.3	30.6	2.7	29.4
B6	4.0	30.9	60.1	29.2	75.45	39.3	30.3	9.0	36.3
	4.5	80.1	99.5	19.4	82.50	38.4	26.0	12.4	36.6
B7	4.5	77.6	65.4	12.3	98.50	66.2	22.5	43.7	45.9
	5.0	76.8	68.3	8.5	99.40	62.6	23.4	39.2	44.9
B8	4.5	85.2	64.9	20.3	85.55	61.7	28.5	33.2	41.0
	5.0	86.8	64.6	22.2	89.55	57.1	25.4	31.7	38.0

Table 8. Results of RTFOT experiments for SBS modified binders

Binder	SBS Content (%)	Mass Loss	After RTFOT		
			Softening Point (°C)	Softening Point Difference (°C)	Permanent Penetration (%)
B4	4.0	0.28	73.65	2.5	88.8
	4.5	0.00	74.50	1.3	91.5
	5.0	0.28	77.45	2.5	91.6
B5	4.0	0.30	81.50	-7.0	82.4
	4.5	0.30	81.50	14.4	87.1
B6	4.0	0.30	76.30	0.8	84.2
	4.5	0.00	84.05	-1.6	85.2
B7	4.5	0.30	99.60	1.7	85.8
	5.0	0.28	96.85	2.7	78.4
B8	4.5	0.30	79.90	-5.6	81.0
	5.0	0.40	78.65	-10.9	71.6

Table 9. Results of DSR and BBR tests for SBS modified binders

Binder	SBS Content (%)	DSR Failure Temp.(°C)	After RTFOT	After RTFOT and PAV	
			DSR Failure Temp.(°C)	DSR Failure Temp.(°C)	BBR Failure Temp.(°C)
B4	4.0	92.8	90.5	16.9	-6
	4.5	95.3	93.1	18.1	-6
	5.0	99.5	92.7	19.8	-6
B5	4.0	89.0	79.7	16.5	-6
	4.5	84.7	78.9	7.0	-6
B6	4.0	85.7	78.9	11.9	-12
	4.5	84.7	80.2	18.6	-12
B7	4.5	106.5	82.4	9.8	-6
	5.0	105.5	82.6	8.9	-6
B8	4.5	88.0	81.1	19.2	-6
	5.0	94.0	88.0	22.8	-6

Table 9 summarizes the results of the DSR and BBR tests of SBS-added binders. The increase in SBS content increased the failure temperatures of B4 and B8 among the unaged binders, while it decreased the failure temperatures of B5, B6, and B7 binders. However, according to the results, the changes in the failure temperatures were limited. After short-term aging, the failure temperatures were found to decrease for all the contents of the SBS modification for all binders. After long-term aging, as the SBS content increased, the failure temperatures of B4, B6, and B8 binders increased, while the failure temperatures for B5 and B7 binders decreased. All results from DSR tests provide the limit values for failure temperatures specified in the PMB technical specification. According to the results of BBR tests, creep hardness values less than 300 MPa and m values greater than 0.300 were reached at -12 °C for the B6 sample and at -6 °C for other binders.

The B4 binder did not achieve the minimum 72 °C softening point limit value suggested for the PMB 82-16 class at 4% SBS content with a very tiny difference when the results of the storage stability tests are not taken into consideration. However, all remaining test results for the B4 binder provide recommended limit values for the PMB 82-16 grade. For mixtures prepared by adding 4.5% and 5% SBS to B4 binder, the recommended limit values for PMB 70-16, PMB 76-16, and PMB 82-16 grades were provided in all test results.

B5 binder could not provide the recommended softening point temperature limit value for PMB 82-16 grade at 4.5% SBS content. In addition, B5 binder could not provide the softening point increase and decrease limit values after RTFOT recommended for PMB 70-16, PMB 76-16, and PMB 82-16 grade binders at 4% and 4.5% SBS content, respectively. However, in all other tests for B5 binder, the recommended limit values were provided for PMB 70-16, PMB 76-16, and PMB 82-16 grade binders at 4% and 4.5% SBS content, respectively.

B7 binder provides the recommended limit values for PMB 70-16, PMB 76-16, and PMB 82-16 grade binders in all test results at both 4.5% and 5% SBS content.

B8 binder provided the recommended limit values in all the remaining tests, except for the after-RTFOT softening point increase/decrease temperature limit values recommended for PMB 70-16, PMB 76-16, and PMB 82-16 class binders at 4% and 4.5% SBS content, respectively.

B6 Binder, on the other hand, provided the required limit values for the BBR test at -12 °C. According to all test results obtained, B6 binder provides all recommended limit values for modified bitumen of PMB 70-22 and PMB 76-22 grades at 4% and 4.5% SBS content, respectively.

4. Conclusions

According to the results of this study, which was conducted to examine the rheological properties of Elvaloy and SBS-added PMBs, which are frequently used in highway construction, it has been determined that PMBs prepared by adding Elvaloy additives at the rates of 1.6%, 1.7%, and 1.8% to B50/70 grade pure bitumen meet the desired specification limit values in all tests. It was determined that PMBs prepared with pure bitumen of B50/70 class by adding 4%, 4.5%, or 5% SBS additives meet the other specification limit values when the storage stability test results are not taken into account. Due to the granular structure of the SBS additive, the fact that the material is not dispersed homogeneously when mixed with pure bitumen is the main reason why the limit values cannot be met in the storage stability experiments. However, as stated in the specification, if the prepared PMB at any polymer additive ratio is to be used in highway construction without being stored, storage stability limit values do not need to be met.

Declaration of Interest Statement

The author declares that he has no known competing financial interests or personal relationships that could have appeared to influence the work reported in this paper.

References

[1] Demir, M. (2011). The Bitumen Modification by Using Reactive Terpolymer and Sbs, Eva. MSc. Thesis. Yıldız Technical University Graduate School of Natural and Applied Science, İstanbul, Türkiye

[2] Luo, W. Q., & Chen, J. C. (2011). Preparation and properties of bitumen modified by EVA graft copolymer. *Construction and Building Materials*, *25*(4), 1830-1835. https://doi.org/10.1016/j.conbuildmat.2010.11.079

[3] Moradı, A. N. (2021). Investigation of Rheological Properties of Bitumen Modified with Diatomites from Seydiler (Afyonkarahisar) Province. MSc. Thesis, Afyon Kocatepe University Graduate School of Natural and Applied Science, Afyonkarahisar, Türkiye.

[4] Choquet, F. (1994). Polymers and modified binders. *Techical Note presented at Belgian Road Research Center*. 1:25-26.

[5] Aydın, H., Yalçın, E., Yılmaz, M. & Alataş, T. (2022) Investigation of Physical and Rheological Properties of Elvaloy and Polyphosphoric Acid Modified Bitumen *Afyon Kocatepe University Journal of Science and Engineering,* 22(5), 1122-1128. https://doi.org/10.35414/akufemubid.1122133

[6] Ilıcalı, M., Tayfur, S., Özen, H., Sönmez, G. & Eren, K., (2001). *Asfalt ve Uygulamaları*. İSFALT Bilimsel Yayınları, Yayın No:1. İstanbul., Türkiye (in Turkish).

[7] Yalçın, H. & Gürü, M., (2002). *Malzeme Bilgisi.* 1. Baskı, Palme Yayıncılık. Ankara, Türkiye (in Turkish).

[8] Cavaliere, M. G., Da Via, M., & Diani, E. (1996). Dynamic-mechanical characterization of binder and asphalt concrete. In *Eurasphalt & Eurobitume Congress, Strasbourg, 7-10 May*.

[9] Isacsson, U., & Lu, X. (1995). Testing and appraisal of polymer modified road bitumens—state of the art. *Materials and structures*, *28*, 139-159. https://doi.org/10.1007/BF02473221

[10] Özdemir, D. K. (2022) Morphological investigation of SBS modified bitumen by innovative microscopies: AFM and CLSM. *Journal of Innovative Transportation*, *3*(2), 29-33. https://doi.org/10.53635/jit.1192375

[11] Jasso, M., Hampl, R., Vacin, O., Bakos, D., Stastna, J., & Zanzotto, L. (2015). Rheology of conventional asphalt modified with SBS, Elvaloy and polyphosphoric acid. *Fuel Processing Technology*, *140*, 172-179. https://doi.org/10.1016/j.fuproc.2015.09.002

[12] Yalçın, E. (2020). Investigation of Rheological Properties of Neat and Modified Binders at Different Temperatures and Frequencies*. BEU Journal of Science*, *9(2)*, 901-909. https://doi.org/10.17798/bitlisfen.597821

[13] Yu, J., Cong, P., & Wu, S. (2009). Laboratory investigation of the properties of asphalt modified with epoxy resin. *Journal of Applied Polymer Science*, *113*(6), 3557-3563. https://doi.org/10.1002/app.30324

[14] Güngör, A. G., Sağlık, A., Orhan, F. & Öztürk, E. A. (2009). Polimer modifiye bitümlerin süperpave performans sınıflarının belirlenmesi. 5. Ulusal Asfalt Sempozyumu. Ankara, Türkiye (In Turkish)

[15] Geçgil, T. & Seloğlu, M. (2019). The Effect of Reactive Terpolymer on The Stiffness and Temperature Susceptibility of Bitumen. *Fırat University Journal of Engineering Science*, 31(1), 203-213.

[16] Kumandaş, E. Ç., Pancar, E. B., & Oruç, Ş. Bitkisel Atık Yağ, RET ve PPA Kompozit Modifiyeli Bitümün Reolojik Özelliklerinin DSR ve BBR ile Araştırılması. IES'20 International Engineering Symposium, December, 5-6 and 10-13, 2020. İzmir, Türkiye

[17] Gedik, A. (2021). Soğuk Bölgelerde Kullanilacak Saf Bitümün Modifikasyonu Ve Beton Asfalt Üretiminde Kullanimi: B70/100 Bitüm Örneği. Adıyaman Üniversitesi Mühendislik Bilimleri Dergisi, 8 (15), 548-559. https://doi.org/10.54365/adyumbd.1001934

[18] TS EN 1426 (2015). Bitumen and bituminous binders - Determination of needle penetration. Turkish Standards Institution

[19] TS EN 1427 (2015). Bitumen and bituminous binders - Determination of the softening point - Ring and Ball method. Turkish Standards Institution

[20] TS EN 13398 (2018). Bitumen and bituminous binders - Determination of the elastic recovery of modified bitumen. Turkish Standards Institution

[21] TS EN ISO 2592 (2017). Determination of flash and fire points - Cleveland open cup method. Turkish Standards Institution.

[22] TS EN 15326+A1 (2010). Bitumen and bituminous binders - Measurement of density and specific gravity - Capillary-stoppered pyknometer method. Turkish Standards Institution.

[23] TS EN 13399 (2018). Bitumen and bituminous binders - Determination of storage stability of modified bitumen. Turkish Standards Institution.

[24] TS EN 14770 (2012). Bitumen and bituminous binders - Determination of complex shear modulus and phase angle - Dynamic Shear Rheometer (DSR). Turkish Standards Institution.

[25] TS EN 14771 (2012). Bitumen and bituminous binders - Determination of the flexural creep stiffness - Bending Beam Rheometer (BBR). Turkish Standards Institution.

[26] ASTM D6648-08 (2016). Standard Test Method for Determining the Flexural Creep Stiffness of Asphalt Binder Using the Bending Beam Rheometer (BBR). American Society for Testing and Materials.

[27] TS EN 12607-1 (2015). Bitumen and bituminous binders-Determination of the resistance to hardening under the influence of heat and air-Part 1:RTFOT method .

[28] AASHTO T 240 (2022). Standard Method of Test for Effect of Heat and Air on a Moving Film of Asphalt Binder (Rolling Thin-Film Oven Test). American Association of State Highway and Transportation Officials.

[29] Sağlık, A., Orhan, F., & Güngör, A. G. (2012). BSK Kaplamalı yollar için Bitüm sınıfı Seçim Haritaları. *TC Ulaştırma Denizcilik ve Haberleşme Bakanlığı Karayolları Genel Müdürlüğü*. Ankara, Türkiye (in Turkish)

JOURNAL OF INNOVATIVE TRANSPORTATION

Internet of things and cloud based smart parking system design criteria

Gul Fatma Turker* iD

a*Department of Computer Engineering, Engineering Faculty, Suleyman Demirel University, Türkiye* ✉

Highlights

- IoT could be used for smart urban transport systems
- RFID, ZigBee and ultrasonic sensors are part of the key sensors
- Cloud-based IoT could be usable tool for parking systems

Abstract

In urban areas, traffic density is seen due to the congested residential areas and the high number of vehicles. The problem of drivers searching for parking spaces in central areas creates traffic. The Internet of Things (IoT) technology offers important solutions with its networking feature to solve problems such as traffic congestion, road safety and inefficient use of parking areas, which are waiting for solutions within the scope of Intelligent Transportation Systems. In this study, the technological infrastructures used by IoT-based smart parking systems are examined and integrated building models are proposed for system designs where parking lots are managed. For smart park design, devices, networks and cloud architecture used in IoT-based systems were examined and requirements were determined. The criteria of an application based on design central management are given. The criteria of an application based on design center management are given. Thanks to the smart parking system to be created in the light of these criteria, the closest parking area will be determined. These designed IoT-based systems will contribute to the reduction of traffic congestion, loss of time in full parking areas, air pollution caused by stop and start vehicles, and fuel savings in the economic field.

1. Introduction

Intelligent transportation systems have been enriched with information and communication technologies as technology progresses. The Internet of Things (IoT) technology has emerged as a tool to increase the efficiency of city services by supporting smart cities in this context. Electronic devices in the digital world equipped with internet connection and sensor networks are interconnected with IoT technology [1,2]. Recently, many IoT-based smart city applications have been developed. Among these applications, there are many studies that overcome challenges such as smart transportation services, road safety, traffic management and vehicle parking [3-7].

Transportation has been one of the basic needs for humanity. The traffic congestion caused by the increasing number of vehicles over time has become an important urban problem by causing high energy consumption and air pollution [8]. Lack of parking spaces is one of the most important causes of traffic congestion. The relationship between congestion and parking arises from the fact that searching for parking spaces causes additional delays and amplifies local circulation. In the center of major cities, 10% of traffic congestion is caused by driving, and it has been found that drivers spend about 20 minutes searching for an empty parking [9].

Urban development faces significant challenges, particularly when it comes to limited parking spaces, and addressing sustainable urban mobility and reducing traffic congestion rank among the most crucial tasks [10]. Cities are becoming smarter through the implementation of data processing techniques, artificial intelligence algorithms, and the integration of various sensors [11-16]. One of the major concerns of today's smart cities is their inability to create adequate and well-managed parking lots to avoid traffic congestion in urban areas.

Raj et al. [17] developed an IoT-based smart parking system for smart cities based on vehicle-to-vehicle communication and vehicle-to-infrastructure communication for autonomous vehicles. They propose a highly automated parking management system that is self-reliant in directing the driver to a nearby parking. The proposed smart parking system has created an electronic device that gathers the parking status information and helps drivers find and select the desired parking spot among the available parking spaces. One study designed a smart parking system that monitors parking spaces, which can be viewed on the website. The system uses MFRC522 for operations, ultrasonic sensor to detect parking spaces, a microcontroller sent to LCD via database to display parking space data on website [18]. Fahim et al. [19] compared a comprehensive technological approach in terms of sensors, network technologies, user interface, computational approaches and service provided in smart parking systems.

With a system design in which the data of IoT-based smart parking systems are transferred over the cloud, systems that inform the drivers in advance of the occupancy status of the parking lots in terms of location, day and time are developed. Canlı and Toklu, A novel mobile smart parking application, leveraging deep learning and cloud-based technology, has been developed to mitigate the issue of parking space search. Within the application, a predictive parking space service utilizing deep learning, specifically Long Short-Term Memory (LSTM), has been devised. Dynamic access to the previously created LSTM-based model is provided via the user's mobile device, and the occupancy rates of the parks are displayed on the mobile device by entering the relevant parameters [20]. Perkovic et al. conducted a study on the actual performance and power consumption of widely used sensor devices and Low Power Wide Area (LPWA) radio technologies (such as LoRa, Sigfox, and NB-IoT) presently accessible. They found that the lowest consumption was for LoRa devices utilizing the IoT system architechtures [21].

There have been many evaluation studies investigating applications, classifying parking systems, revealing smart parking sensors and technologies supported by IoT technology on smart parking systems [3, 22-28]. Similar sensors and communication protocols used in studies covering the application of IoT technology in different areas and current systems designed are shared in the literature [29-34].

According to the literature review given, instant data from the parking areas can be followed with various sensors. In addition, if an IoT-based structure is created, data can be transferred over a network. In this context, data is actively transferred to the cloud over the network connected to the technological infrastructure used in the parking areas, and a system that can be monitored remotely is designed and studies are carried out to provide solutions. In this study, current IoT-based technologies used in smart parking systems were investigated. Considering the differences in the technological infrastructure used in the parking areas, the criteria for integrating into cloud structures are given. Requirements and suggestions have been presented about the creation of designs that enable the control and monitoring of these systems by the center. It is clear that park management center designs, which provide solutions to traffic congestion in urban areas thanks to IoT technology, will become widespread with the arrangement of existing infrastructures in an integrated way.

2. Internet of Things

The term Internet of Things, coined by British technology pioneer Kevin Ashton, co-founder of the Auto-ID Center at the Massachusetts Institute of Technology in 1999, has become increasingly common [35]. This technology makes it possible to network everything around us and communicate with each other with less human intervention. IoT is defined as the connection of things in the physical world or an environment to a network with wired or wireless connections by connecting them with sensors or any embedded system. These connected devices are called smart devices or smart objects. And it consists of intelligent machines that communicate, interact with other machines, the environment, objects. Data can be processed using some processors such as network processor, hybrid processor MCU/MPU. Devices are connected using some technologies such as GPS, Wi-Fi, BT/BTLE, RFID [36]. Devices can be monitored and controlled using remote computers connected over the internet.
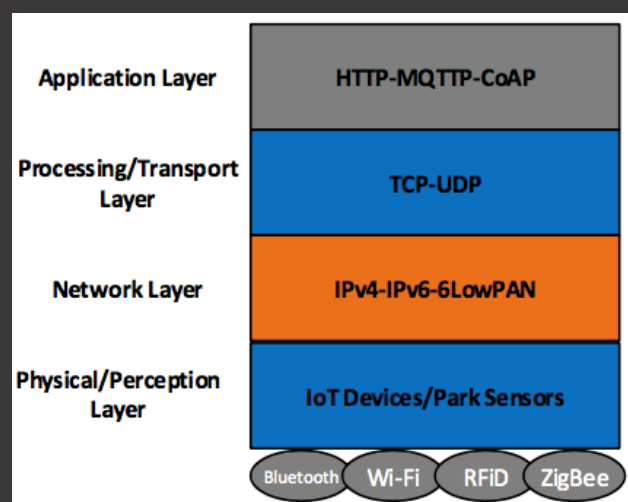

Figure 1. Sample figure and caption

An IoT architecture offers a comprehensive perspective on functionality and connectivity in an IoT ecosystem. Due to the constrained capabilities of IoT devices, authorization solutions specifically designed for IoT environments are frequently implemented in middleware. A four-layer IoT architecture model consisting of physical, network, middleware and

application layers is given in Figure 1. The main functions of the layers are;

Application Layer: It is the top layer of the architectural stack that enables a participant to interact with the system. It encompasses Application Programming Interfaces (APIs) that facilitate communication with middleware, as well as user interfaces that enable end users to access services. Users can search and book their preferred parking spaces using a mobile app or web app. Likewise, parking service providers have the capability to transmit their parking-related information to the integrated system. As users engage directly with the integrated system, this layer delivers the ultimate service to end users.

The predominant protocol in the application layer is Hyper-Text Transfer Protocol (HTTP), which operates over Transmission Control Protocol (TCP) and User Datagram Protocol (UDP). Nonetheless, HTTP is known for its verbosity, complexity, and substantial parsing overhead. As a result, it may not be well-suited for resource-constrained devices in IoT systems. Consequently, several alternative application layer protocols have been devised [37].

The Constrained Application Protocol (CoAP) [38] stands out as one of the extensively adopted protocols for IoT devices, employing a client-server model and operating over UDP. It facilitates asynchronous message exchange and boasts minimal header overhead, simplifying message parsing [39]. Another prevalent application layer protocol is the Message Queue Telemetry Transport (MQTT), which operates above Transmission Control Protocol/Internet Protocol (TCP/IP) as a messaging protocol. MQTT is primarily employed for communication with remote locations where network bandwidth may be limited. However, due to its dependency on TCP, it may not be suitable for real-time processing applications. The Extensible Messaging and Presence Protocol (XMPP) [40] is another widely utilized application layer protocol in IoT. It is designed for streaming Extensible Markup Language (XML) elements and facilitating real-time exchange of structured data.

Middleware layer serves the purpose of facilitating connectivity and interoperability within the IoT ecosystem. It comprises intermediate nodes responsible for processing data received from lower layers and forwarding it to the application layer. The role of middleware in the IoT ecosystem often entails enabling connectivity, interoperability, storage, and data computation. Various types of middleware solutions have been proposed for IoT [41-42]. A comprehensive literature review of IoT reveals that many existing solutions are predominantly based on cloud computing and edge computing as middleware [43]. Cloud computing holds a central position in most IoT platforms, offering flexible and scalable data storage and processing capabilities. The role of the cloud in IoT architecture varies based on the specific application needs and requirements.

The network layer in an IoT ecosystem serves the purpose of facilitating network support and data transfer between nodes [44]. It is responsible for implementing communication protocols required for seamless data exchange. The prevalent network layer protocols utilized in IoT systems are IPv4 and IPv6. IPv6 mandates a minimum MTU (Maximum Transmission Unit) size of 1280 bytes, whereas the IEEE 802.15.4 link layer permits a maximum frame size of 127 bytes. Consequently, supplementary protocols are necessary to enable packet compression for transmitting IPv6 packets over IEEE 802.15.4.

The IPv6 over Low Power Wireless Personal Area Networks (6LoWPAN) [45] protocol is designed to operate on the Low-Rate WPAN specification. It utilizes encapsulation and header compression techniques to facilitate the transmission of IPv6 packets over IEEE 802.15.4 networks. This enables the establishment of a mapping between the link and network layers. The primary objective of 6LoWPAN is to provide IP support for low-power IoT devices. Additionally, Thread7 is another network layer protocol specifically tailored for device-to-device communication in building automation. It is based on IPv6 and 6LoWPAN, offering a comprehensive solution for building automation networks.

IoT systems further expand upon the architectures and protocols utilized in Wireless Sensor Networks (WSN) by incorporating web resources. WSN represents a specific type of IoT network architecture known as a Low-Power and Lossy Network (LLN). In LLN, both devices and routers possess constrained memory and processing capabilities. RPL [46] is an IPv6 routing protocol designed specifically for LLN, efficiently routing various types of traffic, including device-to-central point, central point-to-devices and inter-device communication.

The network layer facilitates communication between the integrated system and users, encompassing parking areas located at various points. It enables the transmission of data from users and parking centers to the integrated system. This layer incorporates diverse communication technologies, including LAN and WAN, for utilization by users, parking service providers, and IoT devices associated with the parking system (e.g., parking sensors and security cameras). It integrates multiple wireless communication technologies such as Lora, Bluetooth, Wi-Fi, along with existing GSM technologies like 4G and 5G. Additionally, this layer ensures scalability and handles the physical layer security of the system.

The physical layer of an IoT system serves to define the sensing and control capabilities. It comprises physical nodes, including sensors and actuators, which detect and

interact with the environment based on changes or user commands [47]. These nodes generate resources that are subsequently transmitted to application nodes through the network and middleware layers. The physical layer encompasses a variety of IoT devices, forming a diverse combination [43].

In IoT ecosystems, different protocols are employed in the physical layer and data link layer, classified based on the type of network they support: Local Area Network (LAN), Personal Area Network (PAN), and Wide Area Network (WAN). Among the commonly used PAN protocols in IoT are Radio Frequency Identification (RFID), Bluetooth, ZigBee, and Z-Wave. RFID is extensively utilized in IoT environments for device identification purposes.

The IEEE 802.15.4 standard is specifically developed for low-speed wireless personal area networks (LRWPAN), providing cost-effective and low-power communication for devices in close proximity. Zigbee is a protocol that is built upon the LRWPAN concept, incorporating additional components for the network and application layers. Similarly, the Z-Wave protocol operates on low-frequency radio bandwidth and is proprietary, not based on a specific standard. Z-Wave encompasses the entire network stack, ranging from the physical layer to the application layer [48].

3. IoT and Cloud Based Smart Parking Systems

Many problems such as vehicle traffic congestion, road safety and ineffective utilization of parking spaces are solved by the IoT technology. When trying to reduce traffic congestion, IoT-based traffic control systems must evaluate all congestion-causing situations. Searching for a parking space can cause traffic congestion and increase Carbon Dioxide (CO_2). In order to find a safe and fast parking spot for drivers in traffic, identifying a parking spot close to its destination and making a reservation in advance has a great effect on reducing congestion.

With IoT-based smart parking systems, the information of empty parking spaces is obtained with the help of sensors and the closest parking location information is sent to the driver. Intelligent systems allow drivers to see their parking spaces and even make online reservations based on their remaining distance to the parking spaces. The needs and infrastructures of smart parking systems should be designed according to the requirements of IoT technology and should be developed in an integrated manner with new technologies. In this section, sensors, network and communication protocols, auxiliary communication technologies used in the infrastructure to be created with IoT technology for smart parking systems are given.

RFID is a communication technology that enables the identification of specific targets and the reading and

writing of relevant data without the need for mechanical or optical contact. This is accomplished through the implementation of the RFID system, also referred to as electronic tags. It is also the largest and fastest developing identity technology widely applied to the IoT. RFID technology can be categorized into energized, de-energized, and semi-powered types. Energized RFID tags are equipped with their own battery, enabling them to have a long read and write distance. However, they tend to be larger in size and come with a higher cost. On the other hand, de-energized RFID tags do not have built-in batteries and rely on power provided by the reader emitter. These tags are smaller in size, more cost-effective, and boast a longer life cycle. They typically have a reading distance ranging from 10mm to 5m, making them widely utilized in applications such as public vehicle cards, food carts, and bank cards [49].

In addition to Wireless Sensor Networks (WSN), RFID is employed to maintain the driver's awareness of the closest parking spot available in the IoT environment. It can be specifically tailored software-driven to gather real-time data on the status of parking spaces. It provides many conveniences to the user, such as the possibility of paying the parking fee via e-wallet. RFID-based systems can easily support extensive parking applications such as parking lot reservation and false parking warning [50].

WSN technology consists of nodes that provide sensing and communication. WSN nodes are usually small and battery powered devices. It easily provides innovative services that facilitate drivers' work quickly and efficiently when searching for an empty parking space nearby in the city. The WSN network architecture can be established by deploying monitoring nodes within parking lots and routing nodes responsible for transmitting the data collected by the monitoring nodes to the base station, forming a tree-like topology. The communication between different sensors and the base station relies on ZigBee technology, enabling short-range communication and minimizing energy consumption [51]. Smart parking reservation applications using ZigBee technology and Bluetooth are being developed. ZigBee sensors are used to detect the vehicle, while Bluetooth communication technique is used to authenticate the driver and also to book a place by identifying free spaces. The Bluetooth range is limited, so if the driver is not active, the connection will be lost and a new slot must be reserved again [52].

ZigBee, renowned for its energy-efficient nature, can operate for extended periods using a single battery. This technology leverages the IEEE standard 802.15.4, offering an impressive outdoor range of 120m and an indoor range of 40m, surpassing the capabilities of Bluetooth and Wi-Fi. Within the smart parking model, each router node utilizes network topology to establish a connection with the main coordinator, enabling direct communication except for the end nodes. ZigBee technology stands out

as a superior choice compared to Wi-Fi and Bluetooth due to its inherent self-orientation and self-healing capabilities. It excels in monitoring and controlling real-time applications, thereby facilitating drivers in locating nearby parking spots, reducing the incidence of accidents, and enhancing vehicle safety. The ZigBee device operates as a transceiver, enabling the acquisition of data from vehicle-detecting sensors and its transmission to the central base station, depending on its operational state [53].

The automatic detection of parking spots, utilizing visual-based methods, relies on the Area View Monitor (AVM) system. Within this system, the mall is strategically positioned to offer an expansive perspective of the parking lot for a single vehicle. The identification of parking spaces is achieved through the implementation of the Line Segment Detector (LSD). Moreover, the AVM employs image segmentation techniques and stereo vision algorithms to effectively identify and navigate around minor obstructions present near parking spaces [54].

The integration of the Fusion Sensor with the AVM and ultrasonic sensors enables the identification of vacant and occupied parking spaces. The process begins with the utilization of various AVM image sequences to detect the markings associated with the parking spaces. Subsequently, the occupancy status of the parking spaces is determined by employing ultrasonic sensors, resulting in the acquisition of relevant information.

The AMR Sensor utilizes Anisotropic Magneto Resistive (AMR) sensors that are deployed within parking slots located alongside the road. The detection of slots is classified as a binary pattern recognition challenge, distinguishing between two states: either occupied (full) or unoccupied (empty).

Ultrasonic Sensor is used together with IoT technology to detect empty and occupied parking spaces. Two ultrasonic sensors are used for each parking space. A specific threshold is established for each sensor to identify the presence of a vehicle within the designated parking space. The parking space is considered occupied only when both sensors detect the presence of a vehicle, thereby indicating its occupancy. These sensors work by emitting higher pitched sounds than the human ear can detect. These sound waves are reflected by nearby objects and send signals back to the sensors. The sensors determine and construct a suitable representation of the surrounding environment by assessing the duration of sound wave reflections from various points within the field.

The Magnetometer Sensor is a device that can seamlessly detect vacant parking lots by measuring the wireless magnetic field change. Parking lot with empty slots is easily detected, mostly using sensors such as

magnetometer and accelerometer to minimize parking search time.

Infrared Sensor is an electronic device that emits light to detect any surrounding object. It detects motion and measures the temperature of the object. The presence and absence of the vehicle is detected by placing IR sensors to find the available parking space.

The accelerometer is among the cellular sensors via smartphones as an accelerometer embedded sensor. It helps to determine whether the driver inside the vehicle is moving the vehicle. At the same time, GPS and gyroscope sensors are used to detect empty parking spaces and create a heat map on the smartphone [25].

Transducer Sensor is a test device that can detect the tested information and convert the detected information into electronic information or other necessary forms.
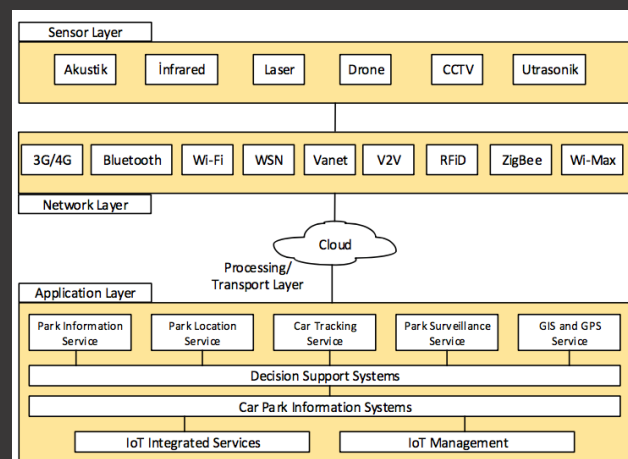

Figure 2. Smart parking system layer and components

In the examples of IoT-based smart parking systems, sensors detailed in this field are used as basic components, and a network is established by selecting the appropriate communication technologies for the system. In Figure 2, the components in the layers as a whole within the scope of the smart parking system are given. When objects are made accessible to the Internet with the designed systems, they can be supported by mobile applications and web applications, and operations such as data collection, data processing and data sharing can be easily provided over a cloud system.

3.1 Cloud design in smart parking systems

A cloud fabric is a model that offers universal, instant network access to a shared pool of customizable computing resources, thereby providing a synonym for a highly available and scalable infrastructure (networks, servers, storage, applications, and services). The Cloud's effectiveness as a model stems from its layered architecture and standardized service models, which are pivotal characteristics contributing to its success. Cloud computing services are offered as Software as a Service

(SaaS), Platform (Platform as a Service-PaaS) and Infrastructure (Infrastructure as a Service-IaaS) [55-56]. IaaS contributes to creating a scalable data center structure by creating infrastructure and virtual server as the basic and flexible cloud model provided by cloud computing technology.

Cloud architecture can be divided into four layers: data center (hardware), infrastructure, platform and application layers. Parking systems, which are considered an important component of ITS for smart cities, should be planned to include all layers. Within this system, it is possible to incorporate an embedded web server, a central web server, sensors, and mobile or web applications specifically developed for parking purposes. Especially in the application part, a parking service should be considered together with supporting cloud applications, web applications and mobile applications.

Based on the state of the parking systems, structures based on the distributed cloud architecture of IoT are being created to improve the process of finding the nearest parking lot in minimum time and to manage the parking systems. Users who have access to the cloud can monitor their reservation information, parking lot location, number, parking fee, distance to the parking lot and availability time as real-time data. In order to prevent the fuel and time spent searching for empty parking spaces, and to prevent traffic jams, a large network is established with the management of the car parks, which are designed as a smart parking system, from a central point.

Steps to be followed in Smart park design created in a cloud system: A designed Cloud-based Smart Parking system should be integrated in all directions. Sensors can be added to the system according to demands, as well as middleware and end-user software that serve the user, variable demands should be presented in a customizable structure for each parking area. With the establishment of an IoT management center, IoT integrated services are connected to the communication layer in the background with a common interface. These are parking lot finding, inspection and information services, GPS services, license plate reading, vehicle tracking services, etc. Common challenges include security, reliability, scale, heterogeneity. Enabling the provisioning of essential resources, storage, and computational power in a transparent and secure manner for vast volumes of diverse and personalized data originating from dispersed sources is accomplished through the advancement of diverse middleware platforms within a finely grained system. Middleware platforms are important so that different IoT ecosystems can communicate with each other.

Within the scope of smart parking systems, different detection technologies can be used in the first layer; laser, infrared, microwave radar, ultrasonic, acoustic sensors or vehicles with video image processing to detect the status of car parks, 3G/4G communication module installed for tracking cars, etc. is selected.

The processing unit acts as an intermediary between the sensors and the cloud. All sensors are wired/wirelessly connected to the processing unit. Data collected from various sensors is sent to the microprocessor, which we call the processing unit. It transmits this data to the server via various protocols over a channel.

In the communication layer, a connection is provided between the application and the sensor layer using various wireless technologies.

At the application layer, the mobile application acts as an interface for web application end users to interact with the system. The application must connect to the server by selecting a secure channel and authorization. The purpose of this developed application includes services such as providing information about the location and availability of parking spaces, and providing the shortest direction. Data transfer takes place between the server and the user application. Platform as a Service (PaaS), Software as a Service (SaaS), Infratructure as a Service (IaaS) services are selected based on different parking services information, processing and storage resources. The cloud acts as a database to store all records regarding parking spaces and end users who have access to the system. It keeps a record of each user connected to the system and can include information such as the time the vehicle was parked, the parking time, the amount paid by the user, and the payment method. It can be structured based on the adaptable essence of the cloud, which permits the system to incorporate an unrestricted count of users at any hour of the day.Continuous backups of data stored in the cloud should also be made so that data can be easily and quickly recovered in case of any system failure.
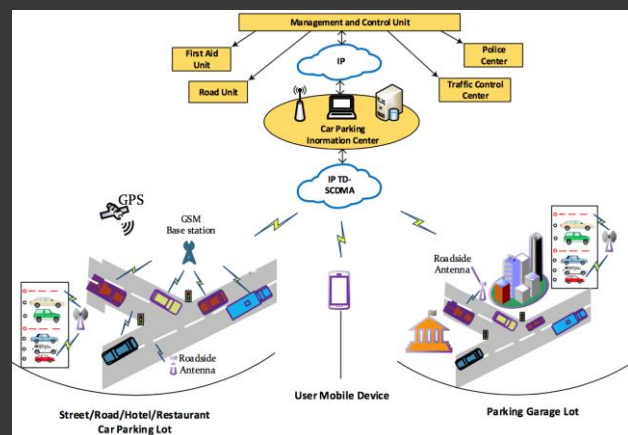

Figure 3. Cloud-based smart parking system and IoT supported smart city architecture

An example design of a smart parking system with centralized management is given in Figure 3. Cloud-based platforms help make it easier to develop and deliver IoT

plugins that enable device to connect to the Cloud. While this service model hides the complexity and heterogeneity of the infrastructure, it also meets the complex requirements for the Cloud such as high activity, scalability, security, easy configurability and flexibility. If there is a demand for smart planning in a city consisting of car parks or indoor car parks in areas such as streets, roads, hotels, restaurants, sensor information is evaluated using multiple communication protocols, and a management system is established by transferring them to the common data center. The data coming to the management center of the system is transferred to the drivers in the fastest way via web or mobile applications.

When cloud-based IoT systems receive a request from the driver looking for the nearest parking spot, the system will process the driver's GPS coordinates and create an area around that location. The system will prepare the road planning that the driver will follow towards one of these parks depending on the traffic situation in this area and the total travel distance between the driver. To get the status of traffic in this area, the number of vehicles on a given route, services such as Road Side Unite (RSU) and Google Traffic can be used. By determining the traffic situation in a certain area, the most suitable route for the driver to reach the nearest parking lot will be created.

4. Conclusion

Smart parking systems and traffic management systems have become reality with the growth of Internet of Things and Cloud technologies. Insufficient parking spaces result in traffic congestion, imbalanced supply and demand, overcrowded parking areas, unfair pricing, on-road and off-road parking, aimless driving, environmental pollution, and deterioration. It has been determined that the presence or knowledge of parking information at the destination to improve the parking facilities of a city and increase the quality of life of the people provides an important solution to the traffic that will be caused by the delay of finding a parking place. Therefore, a parking space estimation system should be developed that can inform the drivers in advance of the occupancy status of the parking lots in terms of location, day and time. In this study, a system design in which the data of IoT-based smart parking systems are transferred over the cloud and the criteria for a system design that provides central management are presented. For smart parking design, devices, networks and cloud architecture used in IoT-based systems were examined and considering the differences in technological infrastructure used in parking areas, requirements and suggestions were given about the features of integration into cloud structures, the creation of designs that allow these systems to be controlled and monitored by the management center.

The cloud structure offers a scalable and flexible data center structure thanks to its configurable computing resources. Within the scope of this study, the technologies used in the creation of IoT and cloud systems are detailed and the necessary criteria for a smart parking system are presented in order to solve the heterogeneity of parking spaces established in different locations and with different technologies. It has been determined that the technological findings revealed as a result of the applications given in the literature review and all the researches are sufficient for the creation of integrated structures for the smart parking system. The recommendations given for the necessary hardware and software selections in an effective design are matched with the literature. Service is provided to users by selecting the most suitable protocols for IoT devices at the application layer. Services such as vehicle information, location, tracking services work in this area. Network and communication protocols and auxiliary communication technologies that provide the connection to the physical layer through the network layer are selected depending on the infrastructure. While using a large number of different sensor technologies created in parking areas as infrastructure, appropriate design suggestions were given to be integrated into the upper layers. Thus, thanks to these cloud-based structures, it contributes to ensuring the regular flow of vehicles in the city without traffic jams, preventing time loss in full parking areas, reducing air pollution caused by vehicles that stop and start, and saving fuel in the economic field.

Declaration of Interest Statement

The author declares that she has no known competing financial interests or personal relationships that could have appeared to influence the work reported in this paper.

References

[1] Centenaro, M., Costa, C. E., Granelli, F., Sacchi, C., & Vangelista, L. (2021). A survey on technologies, standards and open challenges in satellite IoT. *IEEE Communications Surveys & Tutorials*, *23*(3), 1693-1720. https://doi.org/10.1109/COMST.2021.3078433

[2] Laghari, A. A., Wu, K., Laghari, R. A., Ali, M., & Khan, A. A. (2022). A review and state of art of Internet of Things (IoT). *Archives of Computational Methods in Engineering*, 29, 1395-1413. https://doi.org/10.1007/s11831-021-09622-6

[3] Zulfiqar, H., Ul Haque, H. M., Tariq, F., & Khan, R. M. (2023). A survey on smart parking systems in urban cities. *Concurrency and Computation: Practice and Experience*, *35*(15), e6511. https://doi.org/10.1002/cpe.6511

[4] Mollah, M. B., Zhao, J., Niyato, D., Guan, Y. L., Yuen, C., Sun, S., Lam, K. Y. & Koh, L. H. (2020). Blockchain for the internet of vehicles towards intelligent transportation systems: A survey. *IEEE Internet of Things Journal*, *8*(6), 4157-4185. https://doi.org/10.1109/JIOT.2020.3028368

[5] Zhang, H., & Lu, X. (2020). Vehicle communication network in intelligent transportation system based on Internet of

Things. *Computer Communications*, *160*, 799-806. https://doi.org/10.1016/j.comcom.2020.03.041

[6] Mendez Mena, D., Papapanagiotou, I., & Yang, B. (2018). Internet of things: Survey on security. *Information Security Journal: A Global Perspective*, *27*(3), 162-182. https://doi.org/10.1080/19393555.2018.1458258

[7] Ushakov, D., Dudukalov, E., Kozlova, E., & Shatila, K. (2022). The Internet of Things impact on smart public transportation. *Transportation Research Procedia*, *63*, 2392-2400. https://doi.org/10.1016/j.trpro.2022.06.275

[8] Afrin, T., & Yodo, N. (2020). A survey of road traffic congestion measures towards a sustainable and resilient transportation system. *Sustainability*, *12*(11), 4660. https://doi.org/10.3390/su12114660

[9] Ali, G., Ali, T., Irfan, M., Draz, U., Sohail, M., Glowacz, A., ... & Martis, C. (2020). IoT based smart parking system using deep long short memory network. *Electronics*, *9*(10), 1696. https://doi.org/10.3390/electronics9101696

[10] Vlahogianni, E. I., Kepaptsoglou, K., Tsetsos, V., & Karlaftis, M. G. (2016). A real-time parking prediction system for smart cities. *Journal of Intelligent Transportation Systems*, *20*(2), 192-204. https://doi.org/10.1080/15472450.2015.1037955

[11] Da Costa, K. A., Papa, J. P., Lisboa, C. O., Munoz, R., & de Albuquerque, V. H. C. (2019). Internet of Things: A survey on machine learning-based intrusion detection approaches. *Computer Networks*, *151*, 147-157. https://doi.org/10.1016/j.comnet.2019.01.023

[12] Ge, M., Bangui, H., & Buhnova, B. (2018). Big data for internet of things: a survey. *Future generation computer systems*, *87*, 601-614. https://doi.org/10.1016/j.future.2018.04.053

[13] Rjab, A. B., & Mellouli, S. (2021). Smart cities in the era of artificial intelligence and internet of things: promises and challenges. *Smart cities and smart governance: towards the 22nd century sustainable city*, 259-288. https://doi.org/10.1007/978-3-030-61033-3_12

[14] Guo, K., Lu, Y., Gao, H., & Cao, R. (2018). Artificial intelligence-based semantic internet of things in a user-centric smart city. *Sensors*, *18*(5), 1341. https://doi.org/10.3390/s18051341

[15] Rejeb, A., Rejeb, K., Simske, S., Treiblmaier, H., & Zailani, S. (2022). The big picture on the internet of things and the smart city: a review of what we know and what we need to know. *Internet of Things*, *19*, 100565. https://doi.org/10.1016/j.iot.2022.100565

[16] Costa, F., Genovesi, S., Borgese, M., Michel, A., Dicandia, F. A., & Manara, G. (2021). A review of RFID sensors, the new frontier of internet of things. *Sensors*, *21*(9), 3138. https://doi.org/10.3390/s21093138

[17] Fantin Irudaya Raj, E., & Appadurai, M. (2022). Internet of things-based smart transportation system for smart cities. In *Intelligent Systems for Social Good: Theory and Practice* (pp. 39-50). Singapore: Springer Nature Singapore. https://doi.org/10.1007/978-981-19-0770-8_4

[18] Anggraini, N., Dwiyanti, S. M., Putri, T. A., Sari, Y. P., Lusambudi, A. C., & Wahyu, A. P. (2022). Implementation Of IoT-Based Smart Parking Using RFID. *Central Asia & the Caucasus (14046091)*, *23*(1), 3668-3675.

[19] Fahim, A., Hasan, M., & Chowdhury, M. A. (2021). Smart parking systems: comprehensive review based on various aspects. *Heliyon*, *7*(5). https://doi.org/10.1016/j.heliyon.2021.e07050

[20] Canli, H., & Toklu, S. (2021). Deep learning-based mobile application design for smart parking. *IEEE Access*, *9*, 61171-61183. https://doi.org/10.1109/ACCESS.2021.3074887

[21] Perković, T., Šolić, P., Zargariasl, H., Čoko, D., & Rodrigues, J. J. (2020). Smart parking sensors: State of the art and performance evaluation. *Journal of Cleaner Production*, *262*, 121181. https://doi.org/10.1016/j.jclepro.2020.121181

[22] Al-Turjman, F., & Malekloo, A. (2019). Smart parking in IoT-enabled cities: A survey. *Sustainable Cities and Society*, *49*, 101608. https://doi.org/10.1016/j.scs.2019.101608

[23] Hassoune, K., Dachry, W., Moutaouakkil, F., & Medromi, H. (2016). Smart parking systems: A survey. In *2016 11th International Conference on Intelligent Systems: Theories and Applications (SITA)* (pp. 1-6). IEEE. https://doi.org/10.1109/SITA.2016.7772297

[24] Lin, T., Rivano, H., & Le Mouël, F. (2017). A survey of smart parking solutions. *IEEE Transactions on Intelligent Transportation Systems*, *18*(12), 3229-3253. https://doi.org/10.1109/TITS.2017.2685143

[25] Khalid, M., Wang, K., Aslam, N., Cao, Y., Ahmad, N., & Khan, M. K. (2021). From smart parking towards autonomous valet parking: A survey, challenges and future Works. *Journal of Network and Computer Applications*, *175*, 102935. https://doi.org/10.1016/j.jnca.2020.102935

[26] Vachhani, S. K., Nimavat, D., & Kalyani, F. K. (2018). A comparitive analysis of different algorithms used in IOT based smart car parking systems. *Int Res J Eng Technol (IRJET)*, *5*(4), 3244-3248.

[27] Diaz Ogás, M. G., Fabregat, R., & Aciar, S. (2020). Survey of smart parking systems. *Applied Sciences*, *10*(11), 3872. https://doi.org/10.3390/app10113872

[28] Nugraha, D., Ahmed, F. Y. H., Abdullah, M. I., & Johar, M. G. M. (2021). Survey of smart parking application deployment. In *IOP Conference Series: Materials Science and Engineering* (Vol. 1108, No. 1, p. 012019). IOP Publishing. https://doi.org/10.1088/1757-899X/1108/1/012019

[29] Sinha, B. B., & Dhanalakshmi, R. (2022). Recent advancements and challenges of Internet of Things in smart agriculture: A survey. *Future Generation Computer Systems*, *126*, 169-184. https://doi.org/10.1016/j.future.2021.08.006

[30] Salih, K. O. M., Rashid, T. A., Radovanovic, D., & Bacanin, N. (2022). A comprehensive survey on the Internet of Things with the industrial marketplace. *Sensors*, *22*(3), 730. https://doi.org/10.3390/s22030730

[31] Muthuramalingam, S., Bharathi, A., Rakesh Kumar, S., Gayathri, N., Sathiyaraj, R., & Balamurugan, B. (2019). IoT based intelligent transportation system (IoT-ITS) for global perspective: A case study. *Internet of Things and Big Data Analytics for Smart Generation*, 279-300. https://doi.org/10.1007/978-3-030-04203-5_13

[32] Botta, A., De Donato, W., Persico, V., & Pescapé, A. (2016). Integration of cloud computing and internet of things: a survey. *Future generation computer systems*, *56*, 684-700. https://doi.org/10.1016/j.future.2015.09.021

[33] HaddadPajouh, H., Dehghantanha, A., Parizi, R. M., Aledhari, M., & Karimipour, H. (2021). A survey on internet of things security: Requirements, challenges, and solutions. *Internet of Things*, *14*, 100129. https://doi.org/10.1016/j.iot.2019.100129

[34] Uysal, E., Elewi, A., & Avaroğlu, E. (2020). Nesnelerin interneti tabanlı akıllı park sistemleri incelemesi. *Euro J. Sci. Technol*, *20*, 360-366.

[35] Kramp, T., Van Kranenburg, R., & Lange, S. (2013). Introduction to the Internet of Things. *Enabling things to talk: Designing IoT solutions with the IoT architectural reference model*, 1-10.

[36] Mangwani, P. (2018). Smart parking system based on Internet of Things. *International Journal of Applied Engineering Research*, *13*(12), 10281-10285.

[37] Zanella, A., Bui, N., Castellani, A., Vangelista, L., & Zorzi, M. (2014). Internet of things for smart cities. *IEEE Internet of Things journal*, *1*(1), 22-32. https://doi.org/10.1109/JIOT.2014.2306328

[38] Shelby, Z., Hartke, K., & Bormann, C. (2014). The constrained application protocol (CoAP) (No. rfc7252)

[39] Sheng, Z., Yang, S., Yu, Y., Vasilakos, A. V., McCann, J. A., & Leung, K. K. (2013). A survey on the ietf protocol suite for the internet of things: Standards, challenges, and opportunities. *IEEE wireless communications*, *20*(6), 91-98. https://doi.org/10.1109/MWC.2013.6704479

[40] Saint-Andre, P. (2011). Extensible messaging and presence protocol (XMPP): Core (No. rfc6120).

[41] Razzaque, M. A., Milojevic-Jevric, M., Palade, A., & Clarke, S. (2015). Middleware for internet of things: a survey. *IEEE Internet of things journal*, *3*(1), 70-95. https://doi.org/10.1109/JIOT.2015.2498900

[42] Sethi, P., & Sarangi, S. R. (2017). Internet of things: architectures, protocols, and applications. *Journal of electrical and computer engineering*, *2017*. https://doi.org/10.1155/2017/9324035

[43] Ravidas, S., Lekidis, A., Paci, F., & Zannone, N. (2019). Access control in Internet-of-Things: A survey. *Journal of Network and Computer Applications*, *144*, 79-101. https://doi.org/10.1016/j.jnca.2019.06.017

[44] Da Xu, L., He, W., & Li, S. (2014). Internet of things in industries: A survey. *IEEE Transactions on industrial informatics*, *10*(4), 2233-2243. https://doi.org/10.1109/TII.2014.2300753

[45] Montenegro, G., Kushalnagar, N., Hui, J., & Culler, D. (2007). *Transmission of IPv6 packets over IEEE 802.15. 4 networks* (No. rfc4944).

[46] Winter, T., Thubert, P., Brandt, A., Hui, J., Kelsey, R., Levis, P., Pister, K., Struik, R., Vasseur, J. P. & Alexander, R. (2012). *RPL: IPv6 routing protocol for low-power and lossy networks* (No. rfc6550).

[47] Aazam, M., Khan, I., Alsaffar, A. A., & Huh, E. N. (2014). Cloud of Things: Integrating Internet of Things and cloud computing and the issues involved. In *Proceedings of 2014 11th International Bhurban Conference on Applied Sciences & Technology (IBCAST) Islamabad, Pakistan, 14th-18th January, 2014* (pp. 414-419). IEEE. https://doi.org/10.1109/IBCAST.2014.6778179

[48] Kim, K., Cho, K., Lim, J., Jung, Y. H., Sung, M. S., Kim, S. B., & Kim, H. K. (2020). What's your protocol: Vulnerabilities and security threats related to Z-Wave protocol. *Pervasive and Mobile Computing*, *66*, 101211. https://doi.org/10.1016/j.pmcj.2020.101211

[49] Abdulkader, O., Bamhdi, A. M., Thayananthan, V., Jambi, K., & Alrasheedi, M. (2018). A novel and secure smart parking management system (SPMS) based on integration of WSN, RFID, and IoT. In *2018 15th Learning and Technology Conference (L&T)* (pp. 102-106). IEEE. https://doi.org/10.1109/LT.2018.8368492

[50] Mainetti, L., Palano, L., Patrono, L., Stefanizzi, M. L., & Vergallo, R. (2014). Integration of RFID and WSN technologies in a Smart Parking System. In *2014 22nd international conference on software, telecommunications and computer networks (SoftCOM)* (pp. 104-110). IEEE. https://doi.org/10.1109/SOFTCOM.2014.7039099

[51] Hilmani, A., Maizate, A., & Hassouni, L. (2018). Designing and managing a smart parking system using wireless sensor networks. *Journal of Sensor and Actuator Networks*, *7*(2), 24. https://doi.org/10.3390/jsan7020024

[52] Thangam, E. C., Mohan, M., Ganesh, J., Sukesh, C. V., & Prof, A. (2018). Internet of Things (IoT) based smart parking reservation system using raspberry-pi. *International Journal of Applied Engineering Research*, *13*(8), 5759-5765.

[53] Qadir, Z., Al-Turjman, F., Khan, M. A., & Nesimoglu, T. (2018). ZIGBEE based time and energy efficient smart parking system using IOT. In *2018 18th mediterranean microwave symposium (MMS)* (pp. 295-298). IEEE. https://doi.org/10.1109/MMS.2018.8611810

[54] Li, L., Li, C., Zhang, Q., Guo, T., & Miao, Z. (2017). Automatic parking slot detection based on around view monitor (AVM) systems. In *2017 9th International Conference on Wireless Communications and Signal Processing (WCSP)* (pp. 1-6). IEEE. https://doi.org/10.1109/WCSP.2017.8170903

[55] Rani, D., & Ranjan, R. K. (2014). A comparative study of SaaS, PaaS and IaaS in cloud computing. *International Journal of Advanced Research in Computer Science and Software Engineering*, *4*(6).

[56] George, A. S., & Sagayarajan, S. (2023). Securing Cloud Application Infrastructure: Understanding the Penetration Testing Challenges of IaaS, PaaS, and SaaS Environments. *Partners Universal International Research Journal*, *2*(1), 24-34. https://doi.org/10.5281/zenodo.7723187

JOURNAL OF INNOVATIVE TRANSPORTATION

Modelling the effects of flexible pavement distresses in the long-term pavement performance database on performance

Ufuk Kırbaş[a,*] iD, Fazlullah Himat[b] iD

[a] *Civil Engineering Department, Engineering Faculty, Ondokuz Mayıs University, Samsun, TURKEY* ✉
[b] *Graduate School of Higher Education, Ondokuz Mayıs University, Samsun, TURKEY* ✉

Highlights

- HMA pavement modeling with LTPP data
- Comparison of nonlinear regression analysis, MARS, and ANN approaches
- Developing the relationship between IRI and ten types of pavement distress
- Modelling performances are very close to each other

Abstract

Evaluating flexible pavement performance is mandatory for managing transport infrastructure. This study focuses on modeling the relationships between international roughness index (IRI) and a total of 10 types of pavement distress, including alligator, block, wheel path length, wheel path longitudinal, non-wheel path longitudinal, transverse crackings, patches, bleeding, raveling areas, and pumping. The data recorded under the Long-Term Pavement Performance was used to develop the models. Data sets covering General Pavement Studies from seven states of the United States were used in modeling. The study used modeling approaches, including nonlinear regression analysis, multivariate adaptive regression splines, and artificial neural networks (ANN), in which IRI was the dependent variable and pavement distress was the independent variable. In the developed models, 0.516, 0.623, and 0.684 regression coefficients values were obtained for nonlinear regression analysis, multivariate adaptive regression splines, and artificial neural networks approaches, respectively. The analysis results have determined that the artificial neural networks technique performs more successfully than the other techniques. The statistical error analyses of the root mean square error, Nash-Sutcliffe coefficient of efficiency, mean absolute error, and normalized root mean square error also showed that the same modeling approach performs more successfully. With these data generated from a universally used database, it has been determined once again that ANN is the most efficient mathematical approach in modeling the relationships between surface distresses and IRI.

Keywords: International Roughness Index, Pavement Distress, Long-Term Pavement Performance, Distress Effect

1. Introduction

Roads are one of the essential parts of a provincial's infrastructure for economic and social growth. Roads are necessary because they link different parts of the country together and make it easier for people and goods to move around. Every year, governments spend billions of dollars developing new roads and repairing and maintaining existing ones. Roads become more valuable as a country grows, especially if there are no other ways to get around, like railways or canals. The increase in annual expenses shows that coordinated efforts are needed to get the most out of these investments [1, 2].

The effectiveness and efficiency of several civil engineering structures mainly depend on their administration. This ensures that such constructions have a long lifespan, serve their intended purpose, and incur the lowest possible cost. A Pavement Management System (PMS) is a collection of planned and directed activities or procedures that maximize the Return on Investment (ROI) relative to the available budget [3].

The PMS is a structure for managing and maintaining roads based on statistical and mathematical methods. In the 1970s, when there were many more roads to keep track of, the idea of "pavement management" began. PMS was first described at the workshop organized in 1980 as a system that finds the best solutions at different

levels of management and keeps pavements in a good state for use. For many years, many authorities, especially The American Association of State Highway and Transportation (AASHTO) and the Federal Highway Administration (FHWA), have been trying to establish and develop PMS in road networks of different scales [4, 5].

The pavement performance is an essential component of any PMS. The measurement, evaluation and prediction of performance are crucial in managing pavements. The term "deterioration" describes the reduction in the performance level of pavements over time. Road pavements will inevitably deteriorate over time due to axle loads transferred from vehicles, environmental effects, materials used and manufacturing quality. These various parameters contribute to the complexity of the operation. Using performance models, the status of the road at any given time can be approximately predicted [6, 7].

The predicted performance plays a significant role at both the management levels (network and project). The entire facility can be planned using performance models to justify the budget and resources. The planning and timing of maintenance work for specific projects depend on when a section falls out of service. This may be predicted with precision using performance models. In addition to the performance and interplay between the infrastructure facility and its user, formulating an acceptable transportation policy and evaluating its economic benefits depend on the performance and interaction [7].

The pavement's roughness can be considered a simple way to measure road users' satisfaction level and a significant indicator in determining the level of performance. It measures the road surface, ride quality, and comfort of drivers and passengers. Increases in pavement roughness are associated with higher fuel consumption, higher costs for car maintenance and repairs, higher emissions of greenhouse gases, and reduced vehicle efficiency. It might cause traffic safety problems that cost millions of dollars annually to repair. The International Roughness Index (IRI) is a universally accepted parameter to quantify pavement roughness, measured with automated, multifunctional measuring devices or tools [8, 9].

Similar studies recorded in the literature can be summarized as follows. Al-Omari and Darter [10] investigated the correlations amongst them IRI, present serviceability rating (PSR), and several pavement distress types, including rutting, deformations, potholes, and cracks. The Long Term Pavement Performance (LTPP) database data were used in their study. Mactutis et al. [11] studied the relationship between distress and roughness using WesTrack Project data. In this study, a correlation was found between the IRI and the initial IRI of the pavement, the extent of fatigue cracking and the average rut depth. Reportedly, the initial IRI has a significant impact on roughness. Fatigue cracks are very sensitive to roughness, but ruts are not so sharp. Dewan and Smith [12] investigated how pavement distress can be used to calculate vehicle operating costs (VOC) directly. They collected data from the California LTPP sites to establish a relationship between IRI and pavement distress. The correlation was determined on the basis of 39 observations at 15.2 m intervals along a 152.4 m test section. However, Lin et al. [13] studied the capability to estimate IRI from pavement distress collected from pavement videos and photos of a camera sited on an Automated Road Analyzer (ARAN) vehicle. 125 road sections, each section 1-kilometer-long of Taiwan's provincial highways and country roads, were surveyed for data collection. This investigation discovered and examined relationships between 10 different distress types. In addition, some analyzes were made in the study on using IRI to measure the correlation between pavement distress severities and types. Aultman-Hall et al. [14] analyzed the correlations between IRI, cracking, and rutting. This research aimed to determine whether these correlations were able for IRI, the more easily measurable variable, to be substituted for the others. The findings showed that although there are statistically significant correlations between cracking, rutting and IRI, these correlations are insufficient for IRI to substitute pavement conditions.

Besides, Hozayen and Alrukaibi [15] presented a methodology for establishing acceptance criteria determining the performance levels to manage pavements. In their studies, they conducted performance tests on rural roads to learn more about surface roughness and pavement distresses. The overall length of this road is 572 kilometres; it has been divided into three segments 390 kilometres, 139 kilometres, and 43 kilometres. The results showed a regression relationship between raveling and roughness for the three roadway segments, with the coefficient of determination (R2) varying from 0.946 to 0.962. Prasad et al. [16] created a model correlating PMGSY road pavement distress with roughness in India. Data concerning pavement distress were obtained at regular intervals of 50 meters. Bump Integrator, calibrated using MERLIN, was used to collect roughness data. Based on the data obtained in the field, a regression equation was created with the IRI and the visual distresses. The maximum value of the determination coefficient (R2) was 0.66. Also, Meegoda and Gao [17] studied the GPS test section roughness data given in the LTPP database over time to create a model that estimates how pavement roughness would change as the pavement ages. They created and normalized a computable correlation between IRI progression, traffic loads transferred to the pavement, structure number, and climatic area. They created a scale of one to five performance levels to quantify the degree of deterioration of asphalt pavements.

Kirbas et al. [18] investigated the correlation between pavement distress and roughness in flexible pavements. It has been shown that a specific amount of surface distress affects the IRI. A mathematical modeling analysis of the correlations between IRI and 32 distresses with 13 surface distress types, and severities was implemented in their models. The modeling techniques included linear regression, multivariate adaptive regression splines (MARS), and artificial neural networks (ANN). It has been confirmed that the ANN technique is the most accurate. Also, Kirbas et al. [19], in another study, created a pavement performance estimation model that estimates the performance of hot mix asphalt (HMA)-coated provincial roads and state highways under the authority of the General Directorate of Highways (KGM) over the next several years. An empirical equation expressing the relationship between PCI and IRI is also proposed in the study.

Reviewing the literature, Chandra et al. [20], Sandra and Sarkar [21], Mubaraki [22], H Joni et al. [23], Yu Qiao et al. [24] and many more researchers seem to have developed mathematical models that determine the relationships between IRI and surface distress. It is understood that many modeling approaches, such as linear and nonlinear regression models, ANN, fuzzy logic, and MARS, are used to develop models in research. Notably, studies have frequently investigated the relationship between IRI and seven types of deterioration, including potholes, raveling, rutting, cracking, patching, corrugation, and depression. In the models generated, performances up to 0.986 were obtained as the determination coefficient (R2).

The LTPP database collects climate, traffic and performance data on over 2500 road sections. Data entries into this database are made randomly due to the field operators' work plans. While some data can be entered annually, others are entered in the study plans every 2 or 3 years. In addition, overlapping data stacks seasonally is quite troublesome. In this study, special efforts were made to ensure that the data collection dates for each surface disturbance and IRI data evaluated were close to each other. The data stack was prepared carefully, considering the date and significance of each data used in modelling and the climate situation at the time of measurement. In this way, a data set suitable for modelling was obtained. In the literature, it is clearly seen that the similarity values are low in studies that utilize the LTPP database, but the dataset is not created with similar precision. In addition, as seen in other studies of the authors of this study, the ANN method has once again been proven to be the most suitable technique for investigating the relationships between surface distortions and IRI.

There are many studies in the literature that investigate the effects of distress that negatively affect driving comfort on IRI and model the relationships. Also, it is seen that there are limited studies that evaluate the types of distress by considering the severity levels such as low, medium and high. Kumar et al. [6], Prasad et al. [16], Meegoda and Gao [17], and similar studies do not consider the severity levels of pavement distress types. On the other hand, it is understood that one or two types of modeling techniques are frequently evaluated in the investigation of relationships. It is noteworthy that in Shrestha and Khadka [9], Al-Omari and Darter [10], Qiao et al. [24] and similar studies, only one or two techniques were used to investigate the similarities between pavement deterioration and IRI. In terms of the modeling techniques evaluated, there are hardly any studies using three or more methods. With many studies conducted today, it has become clear which parameters affect the estimation of the service level provided by pavements to road users. It is now understood that the research topic focused on is the correct selection of the modeling approach to be used in developing relationships. For this reason, using many techniques in researching relationships and bringing their comparative results to the literature will undoubtedly provide convenience to researchers in solving the problems. Within the scope of this study, the relationships between IRI and a total of 22 independent variables at different severity levels were investigated in 10 various distresses, alligator cracking, block cracking, wheel path longitudinal cracking, non-wheel path longitudinal cracking, transverse cracking, patches area, bleeding area, raveling area, pumping and bleeding, and wheel path length crack, and 6 of them were low, medium and high severity levels, using LTPP data. Three techniques, Nonlinear Regression Analysis, MARS and ANN, were used to investigate the relationships. The working principle established in the study can be seen in the flowchart in Figure 1.
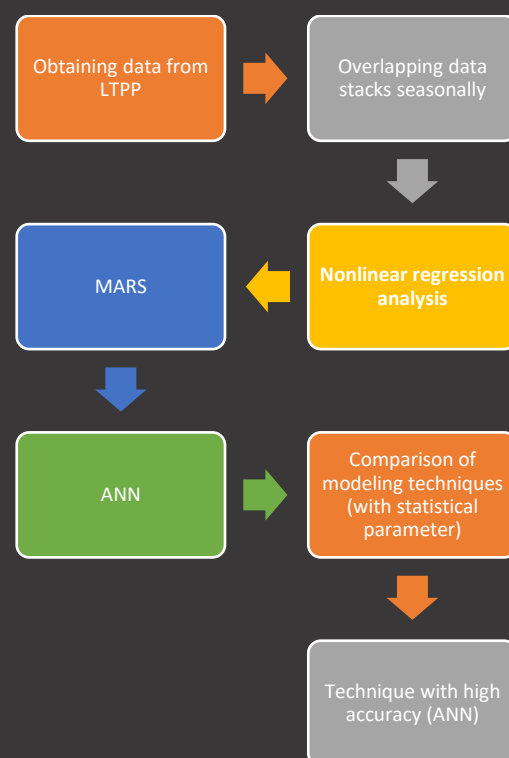

Figure 1. Flowchart of the study

2. Introduction

2.1. Long term pavement performance (LTPP)

The LTPP programme, which has collected data from more than 2581 road segments in the United States and Canada over the past 33 years, is the largest pavement performance research programme. The goal of the LTPP programme is to monitor the performance of pavements in these sections over the long term. The data collected includes information about construction, pavement structure, material quality, maintenance and rehabilitation activities, pavement conditions, pavement loading, and environmental conditions. The LTPP database was developed to record the pavement's characteristics, condition, maintenance activities and reconstruction projects over some time. Each road in the database has a section number indicating where it is located, what material it is made of and how thick the structure is.

Utilizing the LTPP database by the Federal Highway Administration (FHWA) is the principal means for amassing and scrutinizing pavement-related information within the United States and Canada. The LTPP program exhibits a broad reach, enabling the assessment of a pavement's extended-term effectiveness in diverse loading and environmental circumstances. Its objective involves identifying how loading, environment, material characteristics, fluctuations, construction quality, and maintenance levels influence the deterioration and functionality of pavements. Furthermore, it endeavours to enhance design methodologies and strategies and formulate equations that facilitate the rehabilitation of existing and newly constructed pavements [25, 26].

The LTPP database is designed so that users can easily access data from many modules, e.g. inventory, maintenance, monitoring, remediation, materials testing, transport and climate. Within the LTPP program, two distinct categories of experiments are incorporated: general pavement studies (GPS) and specific pavement studies (SPS). These experiments encompass different research approaches and objectives to investigate and analyze various aspects of pavements comprehensively. The general pavement studies (GPS) entail a broader scope, aiming to understand and evaluate pavements' overall performance and behavior under diverse conditions. In contrast, specific pavement studies (SPS) concentrate on more focused research inquiries, targeting particular aspects or phenomena within pavement systems; by combining GPS and SPS, the LTPP program endeavours to provide a comprehensive understanding of pavements, encompassing their overall performance and specific factors and phenomena that influence their functionality and deterioration.

Access to the LTPP data is available through both online and offline means. Starting from March 2003, the online

LTPP data have been accessible via the http://www.infopave.com website. This study uses data from the LTTP InfoPave website [26].

2.2. Data collection

The LTPP database is this study's main data source, containing data up to 2023. The LTPP database's accuracy is acceptable and has been used in several studies. The LTPP data set consists of a classified collection of information from different types of pavement. The data collection includes comprehensive details on the types of pavement, the environment, traffic, maintenance, and rehabilitation. Therefore, LTPP sites located in Arizona, Florida, Minnesota, Mississippi, North Carolina, Oklahoma, and Tennessee from seven states of the United States have been selected to obtain the necessary data according to specific criteria [26].

The LTPP InfoPave website's 'Data' tab was used to obtain the data. A filtering tool allows the selection of only the relevant data. Data was selected, then extracted into a Microsoft Excel file that could be downloaded. In this study, the extracted Excel file for both the IRI and distress tables had the same fields, such as State_Code, SHRP_ID, Survey_Date, and Construction_Number. In this study, the distress data used were obtained from the LTPP table MON_DIS_AC_REV, and IRI data from the LTPP table MON_HSS_PROFILE_SECTION, respectively, and downloaded from the LTPP InfoPave website.

This research selected asphalt concrete pavement on a granular base (GPS-1) and asphalt concrete pavement on a bound base (GPS-2) test sections because these are commonly constructed pavement types. 102 LTPP test sections were selected from GPS–1 and GPS–2, as shown in Table 1. We consider only asphalt concrete (AC) pavements that did not undergo maintenance or rehabilitation at the measurement time. The data collection step was then started. The performance of pavements captured in the LTPP database can be influenced by numerous factors, which can be categorized into four primary domains: structure, climate, traffic, and performance. However, this study selected some factors considered the most important to pavement performance problems, especially the IRI and pavement distress.

Table 1. Presents the final number of test sections in each LTPP state for GPS-1 and GPS-2 pavements

State Code	State Name	Section Total
4	Arizona	17
12	Florida	20
27	Minnesota	13
28	Mississippi	13
37	North Carolina	16
40	Oklahoma	10
47	Tennessee	13
	Total Sections	102

The primary aim of this study is to construct empirical models capable of predicting the behavior of flexible pavements in granular base sections. A multitude of internal and external factors can influence the formulation of the pavement performance model. When constructing or evaluating pavements, it is crucial to take these factors into account to anticipate the long-term functional and structural conditions of the pavement.

The selection of independent variables is determined by considering the structure and accessibility of the LTPP data, its limitations, previous research utilizing the LTPP data, as well as engineering knowledge and expertise. Therefore, the independent variables used for this study are Alligator Cracking (Low), Alligator Cracking (Medium), Alligator Cracking (High), Block Cracking (Low), Block Cracking (Medium), Block Cracking (High), Wheel Path Longitudinal Crack (Low), Wheel Path Longitudinal Crack (Medium), Wheel Path Longitudinal Crack (High), Non-Wheel Path Longitudinal Crack (Low), Non-Wheel Path Longitudinal Crack (Medium), Non-Wheel Path Longitudinal Crack (High), Transverse Crack (Low), Transverse Crack (Medium), Transverse Crack (High), Patches (Low), Patches (Medium), Patches (High), Bleeding Area, Raveling Area, Pumping and Bleeding Length, Wheel Path Length Cracked. The designated dependent variable is the International Roughness Index (IRI).

3. Research Analysis Results

Pavement performance modeling is an essential part of the pavement management system (PMS), which aims to accurately estimate the requirement for pavement maintenance, rehabilitation, or reconstruction. These models estimate how the pavement will be in the future so that maintenance treatments can be made better, and we can see how maintenance operations might affect the future condition of the pavement. Improving the prediction accuracy of estimating methods would result in a more efficient allocation of financial resources, substantial cost savings, and the systematic selection of various maintenance treatments. Researchers have made several models that can predict how well flexible pavements will work using data from extensive experiments in different parts of the world.

The main goal of this study is to use LTPP data from seven states of the United state (Arizona, Florida, Minnesota, Mississippi, North Carolina, Oklahoma, and Tennessee) to build empirical pavement performance models. The relationship between the dependent variable IRI and the independent variable, pavement distress, was studied using regression analysis. In order to identify the best model, regression analysis used three techniques: Nonlinear Regression Analysis, MARS, and ANN.

3.1. Nonlinear regression analysis

Regression analysis is commonly used to estimate the dependent variable given the values of the independent variables. The regression function, which is a function of the independent variables, is the estimation target. Mainly, regression analysis explains how the mean value of the dependent variable changes due to changes in the independent variables. Essential goals of regression analysis include fitting the model to the data and determining the model's adequacy. The quality of the fit is evaluated, resulting in either modification of the model or adoption of the model. Regression analysis is a set of statistical approaches for determining how a dependent variable relates to one or more independent variables. There are three most common types of regression analysis, linear, multiple linear, and nonlinear regression. Most models are either linear or nonlinear. Nonlinear regression analysis is frequently applied to more complex data sets where the relationship between the dependent and independent variables is nonlinear. Linear regression models have parameters that look like they move in a straight line, while nonlinear regression models have at least one parameter that moves in a way that does not look like a straight line. In general, engineering models are nonlinear models. This is because the response of some variables is nonlinearly dependent on the implementation of some independent factors. Nonlinear regression analysis was used to develop the relationship between the international roughness index as a dependent variable and pavement distress as an independent variable, which is the main goal of this research. The Statistical Product and Service Solutions (SPSS) program develops the nonlinear regression model [3, 27].

This study used data from the General Pavement Studies (GPS-1 and GPS-2) to choose 102 test sections to be analyzed. With the help of nonlinear regression analysis modeling, the mathematical relationship between the IRI and 10 types of pavement distress was studied. There are six types of pavement distress, including Alligator Cracking, Block Cracking, Wheel Path Longitudinal Crack, Non-Wheel Path Longitudinal Crack, Transverse Crack, and Patches area with three severity levels: low, medium, and high, and four types of pavement distress have a single severity level, including Bleeding Area, Raveling Area, Pumping and Bleeding Length, Wheel Path Length Cracked. The nonlinear regression analysis was developed at a 0.05 significant level to create the model. The results of the nonlinear regression analysis are shown in Tables 2 and 3.

Table 2. ANOVA results

ANOVA			
Source	Sum of Squares	df	Mean Squares
Regression	1145.772	23	49.816
Residual	142.054	614	0.231
Corrected Total	293.451	636	

Table 3. Model summary

R	R^2	Adjusted R^2
0.718	0.516	0.497

The above result was obtained using the SPSS software and nonlinear regression analysis. Table 3 and Figure 2 summarizes the created model, including the correlation coefficient (R), determination coefficient (R2), and adjusted determination coefficient. The ANOVA table is shown in Table 2.

The dependent variable in the model is the international roughness index, while the independent variable is pavement distress. It is mathematically formulated as Equation (1).

$$
IRI = \begin{bmatrix}
0.972 + \text{Alligator Cracking (L)} \times 6.115\text{E-5} \\
+ \text{Alligator Cracking (M)} \times 0.001 \\
+ \text{Alligator Cracking (H)} \times 0.001 \\
+ \text{Block Cracking (L)} \times 0.001 \\
+ \text{Block Cracking (M)} \times 0.002 \\
+ \text{Block Cracking (H)} \times 0.001 \\
+ \text{Wheel Path Longitudinal Crack (L)} \times 0.003 \\
+ \text{Wheel Path Longitudinal Crack (M)} \times 0.004 \\
- \text{Wheel Path Longitudinal Crack (H)} \times 0.029 \\
- \text{Non Wheel Path Longitudinal Crack (L)} \times 0.001 \\
- \text{Non Wheel Path Longitudinal Crack (M)} \times 0.001 \\
+ \text{Non Wheel Path Longitudinal Crack (H)} \times 0.001 \\
+ \text{Transverse Crack (L)} \times 0.002 \\
+ \text{Transverse Crack (M)} \times 0.004 \\
+ \text{Transverse Crack (H)} \times 0.025 \\
+ \text{Patches Area (L)} \times 0.014 \\
+ \text{Patches Area (M)} \times 0.040 \\
+ \text{Patches Area (H)} \times 0.009 \\
+ \text{Bleeding Length} \times 0.001
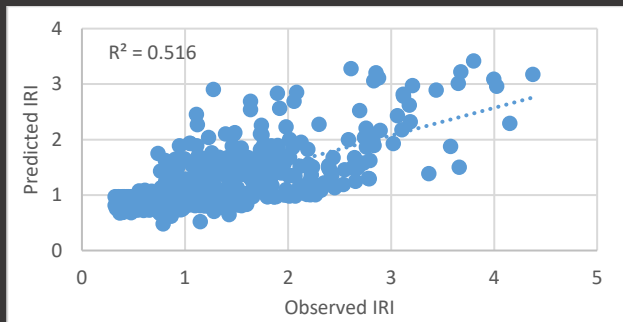\end{bmatrix}
\quad (1)
$$

Figure 2. SPSS model prediction accuracy

3.2. Multivariate adaptive regression splines (MARS)

Multivariate Adaptive Regression Splines (MARS) is also known as the MARS method, which comes from the four letters of its name. Friedman was the first to propose this method [28]. MARS is a non-parametric technique that makes no assumptions about the basic functional relationship between dependent and independent variables. However, it develops a dynamic relationship between cause-effect variables. The MARS technique investigates the relationships between each independent variable and the dependent variable and the interactions between independent variables. It shows the effect of the interactions between all independent variables on the dependent variable. The results of the technique vary based on the number of degrees and modeling terms used [18, 28].

Consequently, it is essential to accurately select these parameters to perform the most effective model analysis. The MARS algorithm is established on the principle of linear partial function expansion with truncation. This situation is represented by Equation (2).

$$[+(X - \tau)]_+, [-(X - \tau)]_+ = [q]_+, [q]_+ \quad (2)$$

Where [q]+ stands for the expression "max (0, q)", and τ stands for a knot with a single variable. The MARS algorithm investigates the relationships between each variable and the locations of knots (nodes) in all feasible partial linear representations [29]. The technique closely follows curve-fitting techniques. The MARS technique has the general form shown in Equation (3).

$$y = \beta_0 + \sum_{j=1}^{P} \sum_{b=1}^{B} \begin{bmatrix} \beta_{bj}(+) \text{Max}(0, X_j - H_{bj}) + \\ \beta_{bj}(-) \text{Max}(0, H_{bj} - X_j) \end{bmatrix} \quad (3)$$

Where P represents the independent variable, and B represents the basic function. These two univariate equations express the basic functions max (0, x− H) and max (0, H − x), and if the β coefficients are 0, just one equation is required. The H values are known as "knots." In contrast to regression analysis, this approach separates the data sets into regions by knots and can deactivate the independent variables under specific conditions and within specified limits. Therefore, it is possible to avoid the occurrence of meaningless result (estimation) values by using the independent variables with extreme values as the model inputs. This has been seen as an important advantage of the MARS approach [18, 30].

The MARS technique uses a stepwise regression process to eliminate basic functions that decrease the model's prediction performance while using a step-by-step progression procedure to investigate the model constants for these basic functions and identify the knots. The generalized cross-validation criterion (GCV) calculates the knot adjustment metric. The GCV criteria are calculated by multiplying the mean residual error by a penalty that is compensated for the variability brought on by the prediction of additional model parameters [31- 33]. GCV formula shown in Equation (4).

$$GCV = \frac{1}{n} \frac{\sum_{i=1}^{n} (y_i - \hat{y}_i)^2}{(1 - P(M)/n)^2} \quad (4)$$

This study used data from the General Pavement Studies (GPS-1 and GPS-2) to choose 102 test sections to be analyzed. With the help of the Multivariate Adaptive Regression Splines (MARS) modeling approach, the mathematical relationship between the international roughness index (IRI) and 10 types of pavement distress

was studied. There are six types of pavement distress, including Alligator Cracking (AC), Block Cracking(BC), Wheel Path Longitudinal Crack (WPLC), Non-Wheel Path Longitudinal Crack (NWPLC), Transverse Crack (TC), and Patches area (PA) with three severity levels: Low (L), Medium (M), and High (H), and four types of pavement distress have a single severity level, including Bleeding Area (BA), Raveling Area (RA), Pumping and Bleeding Length (PBL), Wheel Path Length Cracked (WPLC). A prediction model was developed between IRI and pavement distress. The mathematical model is shown in Equation (5).

$$IRI = \begin{bmatrix} 2.8704736 + 0.0190581 \times BF1 \\ -0.0517728 \times BF2 - 0.0019054 \times BF3 \\ -0.0042911 \times BF4 - 0.0285172 \times BF5 \\ -0.0212036 \times BF6 + 0.0020690 \times BF7 \\ +0.0073641 \times BF8 - 0.0036871 \times BF9 \\ -0.0262217 \times BF10 + 0.0130658 \times BF11 \\ -0.0137322 \times BF12 + 0.0018260 \times BF13 \\ -0.0031871 \times BF14 + 0.0339321 \times BF15 \\ -0.0136603 \times BF16 - 0.0384471 \times BF17 \\ +0.0074482 \times BF18 - 0.0216615 \times BF19 \\ +0.0061849 \times BF20 + 0.0291398 \times BF21 \\ +0.0279002 \times BF22 + 0.0247000 \times BF23 \\ +0.0010227 \times BF24 - 0.0028995 \times BF25 \\ -0.0025667 \times BF26 + 0.0033225 \times BF27 \\ +0.0123699 \times BF28 - 0.3345593 \times BF29 \\ +0.0962880 \times BF30 - 0.0231241 \times BF31 \\ +0.0056054 \times BF32 \end{bmatrix} \quad (5)$$

The mathematical model has 32 basic functions, 22 independent variables, and only one dependent variable. A GCV error of 0.215327 and a threshold of 0.0005 were used to conduct the model analysis. The model's variables are represented by basic functions (BF), which are shown in Table 4.

The regression coefficient (R^2) for this model, which measures how well it can predict, was found to be 0.623109. This model's regression coefficient is 0.623109, which indicates that 62.3% of the IRI variation can be related to the variance of pavement distress. Table 5 shows the statistical regression values of the developed model. The IRI values measured and estimated through the model are comparatively shown in Figure 3.

3.3. Artificial neural networks (ANN)

Artificial Neural Networks (ANNs), or simply neural networks, are one of the intelligent modeling approaches for processing information that may be used for analyzing the interactions among the variables. It is a generalized mathematical model that works like the human brain, which is composed of interconnected neurons of the organic nervous system [34]. In 1943, McCulloch and Pitts introduced the concept of artificial neural networks, but until 1986 when Rumelhart et al. developed the backpropagation algorithm, ANNs gained wide acceptance. ANNs are one of the most popular Artificial Intelligence (AI) approaches.

Table 4. Basic functions used in the MARS model

BF1 = max (0; TC – H – 7.0999999)
BF2 = max (0; 7.0999999 - TC – H)
BF3 = max (0; AC – M - 165.3000031)
BF4 = max (0; 165.3000031 - AC – M)
BF5 = max (0; WPLC – L - 29.8999996)
BF6 = max (0; 29.8999996 - WPLC – L)
BF7 = max (0; BC – M - 114.8000031)
BF8 = max (0; 23.2999992 – NWPLC – L)
BF9 = max (0; P&BL - 17.0000000)
BF10 = max (0; 17.0000000 - P&BL)
BF11= max (0; PA – L - 0.0000000)
BF12 = max (0; NWPLC – H - 150.3999939)
BF13 = max (0; BC – H - 0.0000000)
BF14 = max (0; 155.1999970 – BC – L)
BF15 = max (0; PA – M - 0.0000000)
BF16 = max (0; TC – M - 8.8999996)
BF17 = max (0; 8.8999996 – TC – M)
BF18 = max (0; PA – H - 0.0000000)
BF19 = max (0; WPLC – H - 0.0000000)
BF20 = max (0; 122.0000000 – AC – L)
BF21 = max (0; TC – M - 31.2999992)
BF22 = max (0; WPLC – L - 43.5999985)
BF23 = max (0; 8.5000000 – WPLC – M)
BF24 = max (0; 248.0000000 – NWPLC – M)
BF25 = max (0; WPLC - 133.6000061)
BF26 = max (0; 133.6000061 - WPLC)
BF27 = max (0; TC – L - 55.2000008)
BF28 = max (0; NWPLC – H - 115.0999985)
BF29 = max (0; WPLC - 302.7999878)
BF30 = max (0; WPLC - 294.2000122)
BF31 = max (0; TC – M - 63.9000015)
BF32 = max (0; AC – L - 31.2999992)

Table 5. IRI Prediction Model Regression Statistical Values

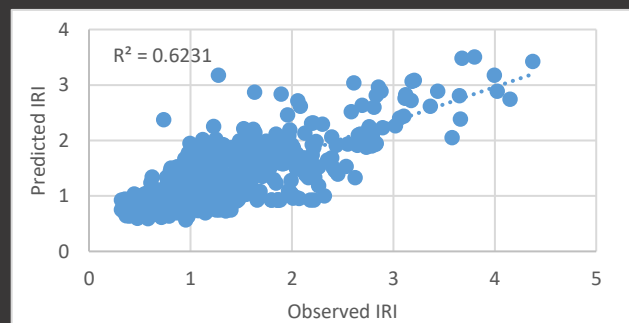| Regression Statistics	IRI
Mean (observed)	1.249411
Standard deviation (observed)	0.679265
Mean (predicted)	1.249411
Standard deviation (predicted)	0.536193
Mean (residual)	0.000000
Standard deviation (residual)	0.417011
R-square	0.623109

Figure 3. MARS model prediction accuracy

AI can be described as the study or process of teaching machines to learn on their own. Artificial intelligence aims to construct machines that work like the human brain and can "think." ANN models are commonly used for prediction and analysis. Even if the sample size is relatively small, models based on artificial neural networks (ANNs) can be used in complicated systems with

multiple interrelated variables. It provides the necessary information by analyzing the stored data. Artificial neural networks (ANNs) copy the human brain using a computer and mathematical processing [20].

ANNs are mathematical systems made up of several neurons connected to one another and have weights assigned to them. An equation commonly referred to as a transfer function is a processing unit. This processing unit gathers and mixes data from other neurons before producing a numerical output. Process units are interconnected in a network and resemble actual neurons. Neural networks are composed of these patterns [19].

The basic structure of an ANN model is usually made up of three layers: the input layer, where known data is added to the model; the hidden layers; and the output layer, where the result of the last search is found. Each layer comprises different parts, called neurons or nodes, with a transfer function connecting it to the layer below it. The number of hidden layers is theoretically unlimited; it should be mentioned [35].

Consider that there are (n) number of input variables in the input node (xi, i = 1, 2,..., n), (p) number of nodes in the hidden layer (zj, j = 1, 2,..., p), and (k) the number of output variables in the output node (ym, m = 1, 2,..., k). The ANN model can be described in Equations (6) and (7).

$$\hat{y}_m = f_y\left(\sum_{j=1}^{p} z_j W_{kj} + b_k\right) \tag{6}$$

$$z_j = f_z\left(\sum_{i=1}^{n} x_i W_{ji} + c_j\right) \tag{7}$$

Where the weight parameters W_{kj} and W_{ji} indicate the strength of the connections between the nodes, b_k, and c_j are the bias functions, and f_y and f_z are the activation functions connected with weight parameters.

The main objective of the ANN model is to optimize the best weight parameters using a training algorithm. The backpropagation technique is most typically used for ANN training, which works by readjusting the weight parameters between the hidden and output layers to minimize output error. There is no exact procedure to determine how many hidden nodes are best, so trial-and-error methods are used to find the best number of hidden nodes. However, it was shown that better outcomes may be achieved when the number of hidden nodes is less than or equal to the number of input nodes. Several activation functions, including the sigmoid, hyperbolic tangent, and sign functions, can also learn nonlinear correlations between the input and output. In ANN modeling, the objective is to create a model that improves accuracy on the training set and then use that model on the test set [36].

In order to figure out the efficiency of ANNs, we divided the input data into three sets. The training data set has

been used to compute gradients to improve network weights. The second set of data, which is used for validation, determines the best neural network training. In reality, the lowest error from the validation phase determines network weights and biases. Regularization can be performed using a validation set to prevent overfitting. After the validation stage of a network, its effectiveness is measured using the test dataset. The training, validation, and testing stages data are randomly selected using various percentages. Training, validation, and testing sets can typically use 70%, 15%, and 15% of the data, respectively [37].

The ANN approach was used in this research for prediction modeling in which pavement distress, including alligator cracking, block cracking, wheel path longitudinal crack, non-wheel path longitudinal crack, transverse crack, patches area, bleeding area, raveling area, pumping and bleeding length and wheel path length cracked were imported as input variables, and IRI was imported as the target variable. A multilayer feed-forward backpropagation network was created and trained with the Levenberg-Marquardt algorithm in MATLAB© software. The number of neurons in the hidden layer can affect the overall number of weights in an ANN model. Selecting a sufficient number of neurons in the hidden layer is important. If the hidden layer has few neurons, the ANN will have less computational resources to deal with the problem. When too many neurons are in the hidden layer, the network can learn insignificant information regarding the training set that is usually unimportant to the overall problem's behavior. Therefore, using the minimum number of neurons in the hidden layer is important.

Figure 4 shows the relationships between the predicted and calculated values using the created ANN model. In this study, the R2 value used to determine the importance of the ANN model developed is 0.684241. The results show that 68.4% of the variance in the IRI could be related to the variance of pavement distress in the developed model.
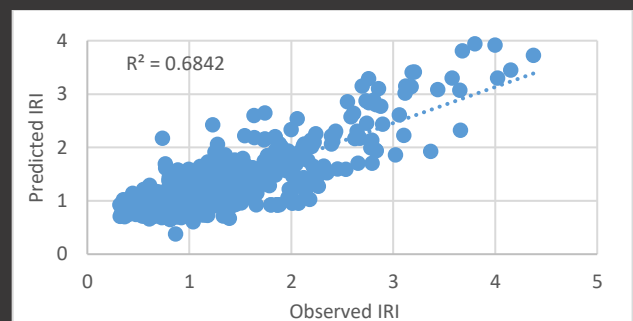

Figure 4. ANN model prediction accuracy

Table 6 shows the structural features of the ANN model developed and calibrated within the scope of the study. As the architecture of the network, there are 22 neurons expressing distress along with severity levels in the input

layer and one neuron expressing IRI in the output layer. Many hidden layers and many neurons were analyzed in the calibration of the network. The highest level of performance was found in 23 neurons in a single hidden layer.

Table 6. Structural details of the ANN model

The structure of the Network used	22 inputs, 23 hidden layers, and 1 output
Percentage of the data used for training, validation, and testing	Training: 70% of the data Validation: 15% of the data Testing: 15% of the data
Type of Network	Feed Forward Back Propagation
Function used for training	Backpropagation
Transfer Function	TANSIG
Training Algorithm	Levenberg-Marquardt
Performance Function	Mean- Squared Error

4. Discussion

In the study, nonlinear regression, MARS and ANN methods were used to model the relationships between inputs and outputs. Briefly, a method progressing from simple to complex was preferred in modelling the relationships between surface distortions and IRI. Besides, nonlinear regression analysis, though relatively interpretable, has limited flexibility in capturing complex relationships between variables. MARS offer adaptability and non-parametric modeling, automatically identifying interactions without distribution assumptions, yet may suffer from increased complexity and potential over-fitting. ANNs excel in capturing intricate non-linear patterns, adaptively learning from data, but their black-box nature, tendency to over fit, and computational demands can limit interpretability and make them resource-intensive. The choice among these approaches hinges on a trade-off: nonlinear regression for interpretability, MARS for a blend of interpretability and adaptability, and ANNs for maximal predictive accuracy while accepting their complexity and computational requirements.

All three mathematical modelling techniques used in the study are solution tools frequently used in science. They have been the subject of numerous studies and scientific publications for years. When you want to examine the recent developments and usage examples of these approaches, you can look at Frost [38] for nonlinear regression, Rodriguez [39] for MARS, and Aggarwal [40] for ANN.

To evaluate more objectively the modeling approaches used in this study between pavement distress and IRI, it is necessary to compare all modeling approaches by using traditional statistical comparison methods such as correlation coefficient (R), determination coefficient (R2), root mean square error (RMSE), Nash-Sutcliffe Efficiency Coefficient (NSCE), mean absolute error (MAE), and

normalized root mean square error (NRMSE). Correlation coefficient in equality (8), determination coefficient in equality (9), root mean square error in equality (10), Nash-Sutcliffe Efficiency Coefficient in equality (11), mean absolute error in equality (12) , and normalized root mean square error are expressed mathematically in Equation (13).

$$R= \frac{\sum_{i=1}^{n}(X_i - \dot{X}) (Y_i - \bar{Y})}{\sqrt{\sum_{i=1}^{n}(X_i - \dot{X})^2 \times \sum_{i=1}^{n}(Y_i - \bar{Y})^2}} \qquad (8)$$

$$R^2= \frac{(\sum_{i=1}^{n}(X_i - \dot{X}) (Y_i - \bar{Y}))^2}{\sum_{i=1}^{n}(X_i - \dot{X})^2 \times \sum_{i=1}^{n}(Y_i - \bar{Y})^2} \qquad (9)$$

$$RMSE= \sqrt{\frac{\sum_{i=1}^{n}(X_i - Y_i)^2}{n}} \qquad (10)$$

$$NSCE=1- \left[\frac{\sum_{i=1}^{n}(X_i - Y_i)^2}{\sum_{i=1}^{n}(X_i - \dot{X})^2}\right] \qquad (11)$$

$$MAE= \frac{\sum_{i=1}^{n}|X_i - Y_i|}{n} \qquad (12)$$

$$NRMSE= \frac{\sqrt{\frac{1}{n}\sum_{i=1}^{n}(X_i - Y_i)^2}}{X_{max}- X_{min}} \qquad (13)$$

Here Xi is the observed value, Yi is the predicted value, $\dot{X}$ is the average of the observed value, $\bar{Y}$ is the average of the observed value, n is the number of samples in the data set, Xmax is the maximum observed value, and Xmin is the minimum observed value. The statistical parameter values found in the three different modeling approaches evaluated in the study are shown in Table 7.

Table 7. Comparison of the model's performance

	MARS	SPSS	ANN
R	0.789372378	0.711546953	0.827188522
R^2	0.623108751	0.506299066	0.684240851
RMSE	0.416683207	0.479350493	0.382164363
NSCE	0.623108751	0.50121841	0.682967028
MAE	0.313949559	0.351148571	0.294739697
NRMSE	0.102757879	0.118212204	0.094245218

These results indicate that the ANN model performs better than MARS and SPSS models. Similar findings were obtained in previous research, confirming that the ANN model's prediction accuracy is satisfactory [7, 8, 41]. The prediction performance of the MARS approach is also better than that of the most used SPSS approaches.

5. Conclusion

Several pavement performance prediction models have been constructed using in-service pavement databases. However, the LTPP database was used in this study because it is the world's largest pavement performance database. The LTPP program is the largest pavement performance research program, collecting data from over 2,581 pavement sections in the United States and Canada over the past 33 years and aiming to study pavement

performance in these sections for a longer period of time. The LTPP program includes two types of experiments: General Pavement Studies (GPS) and Specific Pavement Studies (SPS).

The models have been developed based on the Long-Term Pavement Performance (LTPP) Database. The LTPP data were derived from GPS-1 and GPS-2 sections for seven U.S. states: Arizona, Florida, Minnesota, Mississippi, North Carolina, Oklahoma, and Tennessee. The main purpose of this study was to create pavement performance models to predict IRI from pavement distress using LTPP data.

In this study, regression analysis was performed to develop models from the data collected to study the relationship between IRI as the dependent variable and pavement distress as the independent variable. To develop the best model, regression analysis is performed using three methods Nonlinear Regression Analysis, Multivariate Adaptive Regression Splines (MARS), and Artificial Neural Networks (ANN).

The developed models have coefficients of determination (R2) equal to 0.516, 0.623, and 0.684 for nonlinear regression analysis, multivariate adaptive regression splines (MARS), and artificial neural networks (ANN), respectively. The models generated, calibrated and put into use within the scope of the study are explained in sections 3.1, 3.2 and 3.3 of the study. Finally, the results showed that the developed ANN model could predict the IRI of GPS-1 and GPS-2 pavement sections with very good accuracy and less error compared to nonlinear regression analysis and multivariate adaptive regression splines (MARS) models. The most valuable statistics error analyses, including R, R2, RMSE, NSCE, MAE, and NRMSE, were employed to compare the developed models are also supported the ANN model for better performance.

The performance levels of mathematical models are evaluated with the benchmark parameters allowed by statistics. In this study, six of these benchmark parameters were used for comparison. According to all these parameters, it is clear that the level of agreement between the prediction results of the models developed with three different techniques and the actual data is highest in the model developed with the ANN approach. This comparison is explained in chapter 4.

Due to the complex structure of fieldwork and the need for intensive labour, surface distress and IRI measurements cannot be made on very recent dates and in a recurring format every year. In addition, although some surface distress data have a negative impact on the mechanical strength of the pavement, their negative impact on surface irregularity (roughness) is limited. Even if some surface distresses are on the coating surface, their effect on discomfort remains limited since they are not on the trace of the IRI measurement. All these constraints are the main reasons prediction similarities remain at limited levels in modelling studies. As a result, the effects of each distress type and severity on IRI can be determined with precision only with similarity models created in a universe where data sets are created under idealized conditions. It is clear that until these idealized conditions are met, repeating similar studies on data produced under actual application conditions will continue to shed light on science.

Declaration of Interest Statement

The authors declare that they have no known competing financial interests or personal relationships that could have appeared to influence the work reported in this paper.

Author Contribution Statement

U. Kırbaş: Conceptualization, Data Curation, Formal analysis, Investigation, Methodology, Project administration, Resources, Software, Supervision, Validation, Visualization, Writing-Original Draft, Writing-Review & Editing; **F. Himat**: Data Curation, Formal analysis, Investigation, Methodology, Software, Validation, Visualization, Writing-Original Draft, Writing-Review & Editing

References

[1]   Solatifar, N., & Lavasani, S. M. (2020). Development of an Artificial Neural Network model for asphalt pavement deterioration using LTPP data. *Journal of Rehabilitation in Civil Engineering, 8(1)*, 121-132. https://doi.org/10.22075/JRCE.2019.17120.1328

[2]   Zaltuom, A. M. A., & Yulipriyono, E. (2011). Evaluation Pavement Distresses using Pavement Condition Index. *Magister Teknik Sipil (Doctoral dissertation).*

[3]   Alsheyari, K. A. O. (2017). A Case Study of Investigation the impact of International Roughness Index in developing pavement deterioration model in the United Arab Emirates. *The British University in Dubai (BUiD)) (Doctoral dissertation).*

[4]   Fang, X. (2017). Development of distress and performance models of composite pavements for pavement management. The University of North Carolina at Charlotte (Doctoral dissertation).

[5]   Heanue, K. (2007). *Integrating Freight into Transportation Planning and Project-Selection Processes (No. NCHRP Project 8-53).* Washington, DC: National Academies Press. https://doi.org/10.17226/23139

[6]   Kumar, R., Suman, S. K., & Prakash, G. (2021). Evaluation of pavement condition index using artificial neural network approach. *Transportation in Developing Economies, 7(2)*, 20. https://doi.org/10.1007/s40890-021-00130-7

[7]   Terzi, S. (2013). Modeling for pavement roughness using the ANFIS approach. *Advances in Engineering Software, 57*, 59–64. https://doi.org/10.1016/j.advengsoft.2012.11.013

[8] Abdelaziz, N., Abd El-Hakim, R. T., El-Badawy, S. M., & Afify, H. A. (2020). International Roughness Index prediction model for flexible pavements. *International Journal of Pavement Engineering, 21(1)*, 88-99. https://doi.org/10.1177/03611981211017906

[9] Shrestha, S., & Khadka, R. (2021). Assessment of Relationship Between Road Roughness And Pavement Surface Condition. *Journal of Advanced College of Engineering and Management, 6*, 177-185. https://doi.org/10.3126/jacem.v6i0.38357

[10] Al-Omari, B., & Darter, I. (1995). Effect of pavement deterioration types on IRI and rehabilitation. *Transportation Research Record, 1505,* 57.

[11] Mactutis, J. A., Alavi, S. H., & Ott, W. C. (2000). Investigation of relationship between roughness and pavement surface distress based on WesTrack project. *Transportation Research Record, 1699*, 107-113. https://doi.org/10.3141/1699-15

[12] Dewan, S. A., & Smith, R. E. (2002). Estimating International Roughness Index from pavement distresses to calculate vehicle operating costs for the San Francisco Bay area. *Transportation Research Record, 1816*, 65-72. https://doi.org/10.3141/1816-08

[13] Lin, J. D., Yau, J. T., & Hsiao, L. H. (2003). Correlation analysis between international roughness index (IRI) and pavement distress by neural network. *Transportation Research Board, 12(16),* 1-21.

[14] Aultman-Hall, L., Jackson, E., Dougan, C. E., & Choi, S. N. (2004). Models relating pavement quality measures. *Transportation Research Record, 1869,* 119-125. https://doi.org/10.3141/1869-14

[15] Hozayen, H. A., & Alrukaibi, F. (2008). Development of acceptance measures for long term performance of BOT highway projects. Al-Qadi, I.L., Sayed, T., Alnuaimi, N., Masad, E., *In Efficient Transportation and Pavement Systems: Characterization, Mechanisms, Simulation, and Modeling,* 347-360. London: CRC Press. https://doi.org/10.1201/9780203881200

[16] Prasad, J. R., Kanuganti, S., Bhanegaonkar, P. N., Sarkar, A. K., & Arkatkar, S. (2013). Development of relationship between roughness (IRI) and visible surface distresses: a study on PMGSY roads. *Procedia-Social and Behavioral Sciences, 104,* 322-331. https://doi.org/10.1016/j.sbspro.2013.11.125

[17] Meegoda, J. N., & Gao, S. (2014). Roughness progression model for asphalt pavements using long-term pavement performance data. *Journal of Transportation Engineering, 140(8)*, 04014037. https://doi.org/10.1061/(ASCE)TE.1943-5436.0000682

[18] Kırbaş, U., & Karaşahin, M. (2016). Performance models for hot mix asphalt pavements in urban roads. *Construction and Building Materials, 116*, 281-288. https://doi.org/10.1016/j.conbuildmat.2016.04.118

[19] Kırbaş, U. (2018). IRI sensitivity to the influence of surface distress on flexible pavements. *Coatings, 8(8),* 271. https://doi.org/10.3390/coatings8080271

[20] Chandra, S., Sekhar, C. R., Bharti, A. K., & Kangadurai, B. (2013). Relationship between pavement roughness and distress parameters for Indian highways. *Journal of Transportation Engineering, 139(5),* 467-475. https://doi.org/10.1061/(ASCE)TE.1943-5436.0000512

[21] Sandra, A. K., & Sarkar, A. K. (2013). Development of a model for estimating International Roughness Index from pavement distresses. *International Journal of Pavement Engineering, 14(8),* 715-724. https://doi.org/10.1080/10298436.2012.703322

[22] Mubaraki, M. (2016). Highway subsurface assessment 2using pavement surface distress and roughness data. *International Journal of Pavement Research and Technology, 9(5),* 393-402. https://doi.org/10.3850/978-981-11-0449-7-329-cd

[23] Joni, H. H., Hilal, M. M., & Abed, M. S. (2020, February). Developing International Roughness Index (IRI) Model from visible pavement distresses. *Materials Science and Engineering, 737(1),* 012119. https://doi.org/10.1088/1757-899X/737/1/012119

[24] Qiao, Y., Chen, S., Alinizzi, M., Alamaniotis, M., & Labi, S. (2022). Estimating IRI based on pavement distress type, density, and severity: Insights from machine learning techniques. *Transportation Reseach Board, 2022.* https://doi.org/10.48550/arXiv.2110.05413

[25] Zeiada, W., Hamad, K., Omar, M., Underwood, B. S., Khalil, M. A., & Karzad, A. S. (2019). Investigation and modelling of asphalt pavement performance in cold regions. *International Journal of Pavement Engineering, 20(8),* 986-997. https://doi.org/10.1080/10298436.2017.1373391

[26] Elkins, G. E., & Ostrom, B. (2021). *Long-term pavement performance information management system user guide (No. FHWA-HRT-21-038).* United States: Federal Highway Administration. Office of Infrastructure Research and Development.

[27] Ross, S. M. (2020). *Introduction to probability and statistics for engineers and scientists.* United States: Academic Press.

[28] Friedman, J. H. (1991). Multivariate adaptive regression splines. *The Annals of Statistics, 19(1),* 1-67. https://doi.org/10.1214/aos/1176347963

[29] Weber, G. W., Batmaz, I., Köksal, G., Taylan, P., & Yerlikaya-Özkurt, F. (2012). CMARS: a new contribution to non-parametric regression with multivariate adaptive regression splines supported by continuous optimization. *Inverse Problems in Science and Engineering, 20(3)*, 371-400. https://doi.org/10.1080/17415977.2011.624770

[30] Attoh-Okine, N. O., Cooger, K., & Mensah, S. (2009). Multivariate adaptive regression (MARS) and hinged hyperplanes (HHP) for doweled pavement performance modeling. *Construction and Building Materials, 23(9),* 3020-3023. https://doi.org/10.1016/j.conbuildmat.2009.04.010

[31] Attoh-Okine, N. O., Mensah, S., & Nawaiseh, M. (2003). A new technique for using multivariate adaptive regression splines (MARS) in pavement roughness prediction. *In Proceedings of the Institution of Civil Engineers-Transport*, 156(1), 51-55. https://doi.org/10.1680/tran.2003.156.1.51

[32] Rounaghi, M. M., Abbaszadeh, M. R., & Arashi, M. (2015). Stock price forecasting for companies listed on Tehran stock exchange using multivariate adaptive regression splines model and semi-parametric splines technique. *Physica A: Statistical Mechanics and its Applications, 438,* 625-633. https://doi.org/10.1016/j.physa.2015.07.021

[33] Zhang, W. G., & Goh, A. T. C. (2013). Multivariate adaptive regression splines for analysis of geotechnical engineering systems. *Computers and Geotechnics, 48*, 82-95. https://doi.org/10.1016/j.compgeo.2012.09.016

[34] Soni, A., Yusuf, M., Beg, M., & Hashmi, A. W. (2022). An application of Artificial Neural Network (ANN) to predict the friction coefficient of nuclear grade graphite. *Materials Today: Proceedings,* 68, 701-709. https://doi.org/10.1016/j.matpr.2022.05.567

[35] Juan, N. P., & Valdecantos, V. N. (2022). Review of the application of Artificial Neural Networks in ocean

engineering. *Ocean Engineering, 259,* 111947.
https://doi.org/10.1016/j.oceaneng.2022.111947

[36]   Kim, T., Shin, J. Y., Kim, H., Kim, S., & Heo, J. H. (2019). The use of large-scale climate indices in monthly reservoir inflow forecasting and its application on time series and artificial intelligence models. *Water, 11(2),* 374. https://doi.org/10.3390/w11020374

[37]   Fakhri, M., & Dezfoulian, R. S. (2019). Pavement structural evaluation based on roughness and surface distress survey using neural network model. *Construction and Building Materials, 204,* 768-780. https://doi.org/10.1016/j.conbuildmat.2019.01.142

[38]   Frost, J. (2020). *Regression Analysis: An Intuitive Guide for Using and Interpreting Linear Models*. U.S.A.: Statistics By Jim Publishing.

[39]   Rodriguez, R.N. (2023). *Building Regression Models with SAS: A Guide for Data Scientists.* Newyork City, U.S.A.: SAS Institute.

[40]   Aggarwal, C.C. (2023). *Neural Networks and Deep Learning: A Textbook.* Newyork City, U.S.A.: Springer International Publishing.

[41]   Kırbaş, U., Karaşahin, M., Demir, B., Komut, M., Ünal, E.N., (2018). Some approaches to the modeling of relationships between surface distresses and roughness in hot-mixed asphalts. *Süleyman Demirel University Journal of Natural and Applied Sciences, 22(2),* 901-912. https://doi.org/10.19113/sdufbed.32804